

Information for users of  
METTLER TOLEDO thermal analysis systems

## Dear Customer,

2005 was once again a successful year for METTLER TOLEDO and for the thermal analysis group in particular. We have introduced many new products and hope that this will enable us to provide you with even better analytical support in future.

**TOPEM**<sup>®</sup> is a completely new patented temperature-modulated DSC technique.

The **STAR**<sup>®</sup> software has also been undergoing continuous development and is now even better optimized for your needs. Some of the new features are the direct result of your feedback and suggestions.

We would like to wish you a successful start into the New Year and look forward to surprising you again with new products.

## Method development in thermal analysis. Part 2:

Dr. Markus Schubnell

Part 1 (Steps 1 to 3) of the TA TIP on method development appeared in UserCom21 (1/2005). This article is the second and final part of this series.

### Step 4: Choosing the temperature program

The two main aspects that have to be considered are the

- Type of temperature program (single segment, multi-segment, modulated temperature program).
- Choice of parameters (heating rate, start and end temperatures, and if relevant, amplitude and period).

Table 4 displays the different temperature programs and gives recommendations for the different TA measurement techniques.

# 22

### Contents

#### TA Tip

- Method development in thermal analysis. Part 2: 1

#### New in our sales program

- **STAR**<sup>®</sup> V9.00 5
- DSC823<sup>e</sup> 5
- **TOPEM**<sup>®</sup> – The new multi-frequency temperature-modulated technique 6

#### Applications

- Estimation of the long-term stability of materials using advanced model free kinetics 8
- Thermal analysis experiments with fire-retarded polymers 12
- The separation of sensible and latent heat flow using **TOPEM**<sup>®</sup> 16

#### Tips and hints

- Simple determination of the thermal conductivity of polymers by DSC 19

#### Dates

- Exhibitions 23
- Courses and Seminars 23

**METTLER TOLEDO**

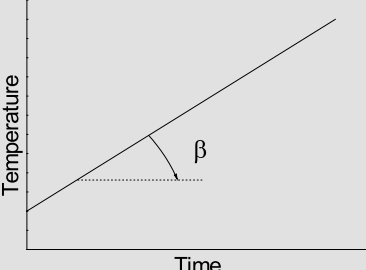
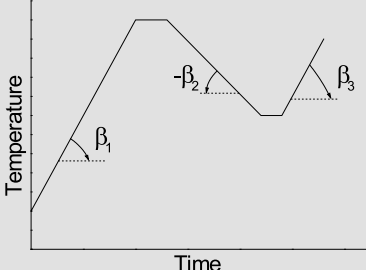
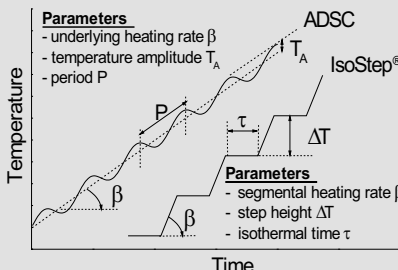
			
	Dynamic heating segment with constant heating rate; this is the usual temperature program	Temperature program consisting of several segments (isothermal, dynamic heating and cooling segments)	Temperature-modulated heating program: ADSC and IsoStep
DSC	Typical heating rate: <b>10</b> to 20 K/min Low heating rates give good resolution at the cost of sensitivity	Simplifies interpretation; heating and cooling rates are typically between 5 and 20 K/min. Thermal pretreatment	Typical parameters ADSC $\beta = 0.5\text{-}2$ K/min $T_A = 0.2\text{-}2$ K $P = 40\text{-}120$ s IsoStep $\beta = 0.5\text{-}2$ K/min $T_A = 0.5\text{-}2$ K $P = 30\text{-}120$ s
TGA	Typical heating rate: 10 to <b>20</b> K/min	Only in special cases	Direct determination of the conversion-dependent apparent activation energy of a reaction
TMA	Typical heating rate: 5 K/min	Facilitates interpretation; heating and cooling rates are typically between 3 and 10 K/min Thermal pretreatment	Separation of thermal expansion and contraction
DMA	Typical heating rate: 3 K/min	Thermal pretreatment	Is not used

Table 4. Overview of different temperature programs and their use.

The heating rate and the start and end temperatures are chosen with the following factors in mind:

- Thermal conductivity of the sample: the temperature distribution in the sample should always be as homogeneous as possible (→ low heating rates).
- The lower the heating rate, the better the temperature resolution.
- The higher the heating rate, the more pronounced the effects (DSC, SDTA).
- Start and end temperatures: the time interval before and after the first and last thermal events should be sufficiently long to enable a clear “baseline” to be drawn. Recommended values: DSC 3 min, TGA: 5 min, TMA: 5 min, DMA 8 min.

In standard methods, for example ASTM and DIN, the temperature program is often specified. According to ISO 17025, such standard methods no longer need to be validated. This should, however, be treated with caution because many stand-

ard methods are not fully validated. In practice, variations of standard methods are often used that most certainly require validation.

### Step 5: Choosing the atmosphere

With DSC and TGA in particular, different atmospheric conditions allow different types of information to be obtained. This is illustrated in Figure 4, which describes the decomposition of coal as an example. The upper curve was measured in an air atmosphere, the lower curve under nitrogen (up to 900 °C) and then air (above 900 °C). In air, the combustion profile of the sample is of interest, that is, the temperature at which the coal begins to burn, and how the combustion process proceeds. If the measurement is first performed in an inert atmosphere and then finally under air, the main questions have to do with the composition of the coal, that is, the content of volatile compounds (moisture, adsorbed gases), whether inorganic compounds are present, and the carbon content.

In DSC, the atmosphere within the crucible plays an important role. For example, in an open crucible, one observes the slow evaporation of solvents and moisture. This process gives rise to broad endothermic peaks that sometimes overlap with other interesting effects such as glass transitions and polymorphic transitions.

If the crucible is sealed with a crucible lid that has been pierced with a small hole, a so-called self-generated atmosphere is created and the evaporation process is delayed almost to the boiling point of the liquid. Above the boiling point, the liquid evaporates rapidly from the crucible. METTLER TOLEDO supplies lids with a hole-diameter of 50  $\mu\text{m}$  for this type of measurement. Finally, in a hermetically sealed crucible, the boiling point can be exceeded. The crucible is then under pressure. This can lead to initial deformation of the crucible and ultimately, on further temperature increase, to bursting (see Figure 5). Endothermic evaporation can

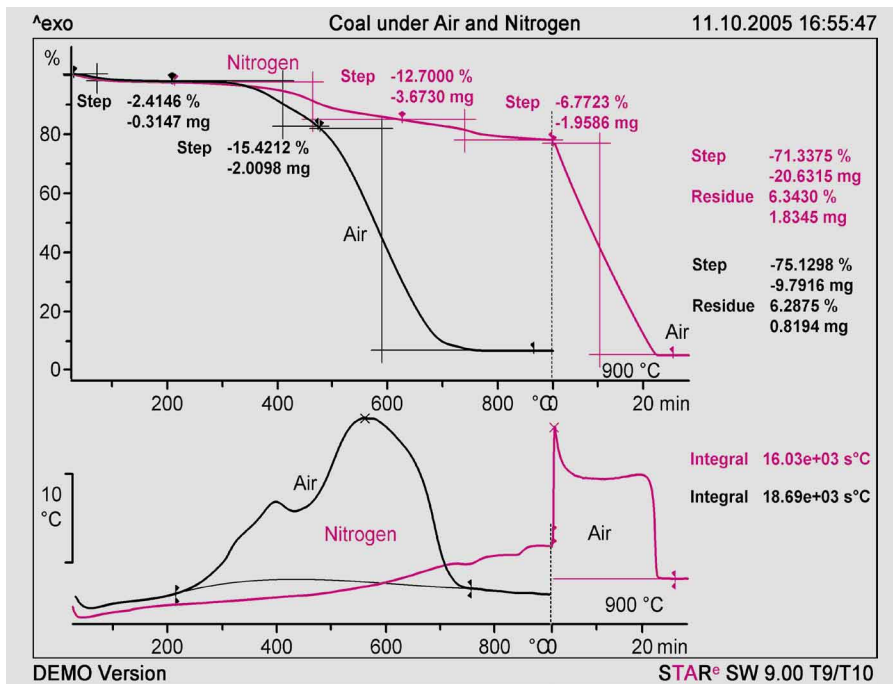


Figure 4. TGA measurements of coal in air and under nitrogen. Measurement in air allows the combustion process of the coal to be followed; heating under nitrogen is used for quantitative compositional analysis.

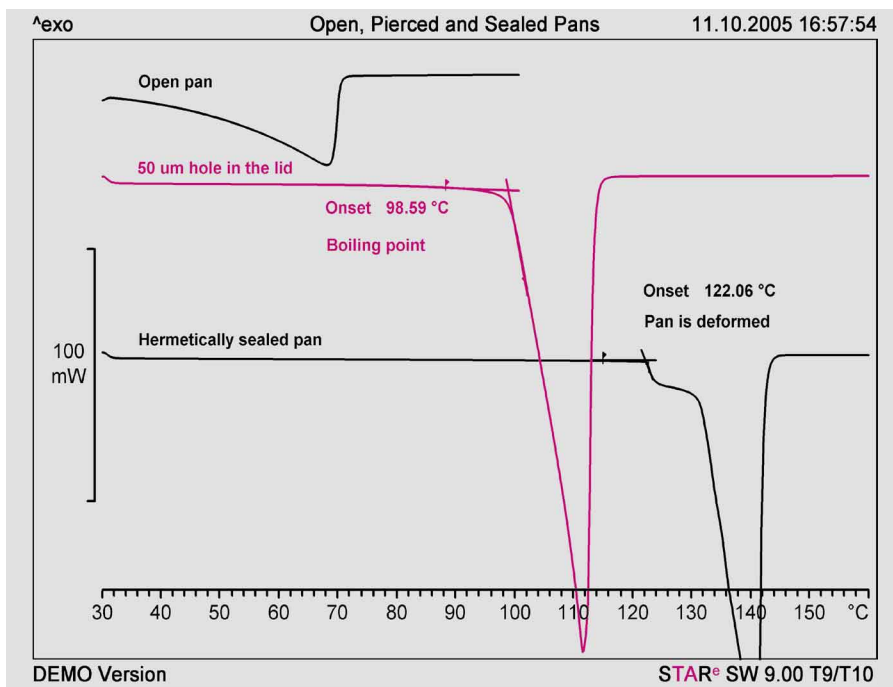


Figure 5. DSC measurements of water in an open crucible, under a self-generated atmosphere and in a hermetically sealed crucible.

be completely suppressed by using medium pressure crucibles.

### Step 6: Examining the sample after measurement

One should make a habit of weighing samples before and after an experiment (even with TMA and DMA measurements). Small

mass changes indicate that evaporation or initial decomposition processes have taken place. This usually has an effect on the measurement curves (not only DSC, but also TMA and DMA curves). These effects are often only weak and may hardly be noticeable so that the gravimetric information is very important.

A further aid to interpretation is a visual examination of the sample after the experiment. Points to check are

- Has the color changed?
- Does the sample appear to have melted?
- Has the sample undergone deformation?

Answers to such questions can lead to a better interpretation and understanding of the effects observed in the measurement curves.

### Step 7: Evaluation

To obtain quantitative results, the measured curves have to be properly evaluated. Often, several different methods (involving the choice of baseline, drawing of tangents, etc) are available to calculate numerical results from the curves. This in turn may lead to different measurement results being obtained. For example, the glass transition temperature can be determined from DSC curves according to ASTM and DIN methods, and according to other procedures (Richardson, bisector of tangents). To meaningfully compare measurement results, it is important to evaluate measurement curves in exactly the same way each time and to state the method used (baseline type, tangent type) to obtain the results.

### Step 8: Validation

Once steps 1 to 7 have been defined, the final task is to design an experimental plan for validation, that is, to plan a certain number of experiments. This includes specifying the number of repeat measurements (for repeatability) that must be performed, as well as defining the order in which sample and reference sample measurements and blank curves must be measured. This also includes giving details about the statistical methods to be used for further analysis of experimental series.

### Conclusions

Method development begins with a trial method that is optimized in steps and finally validated. A good trial method can greatly facilitate the method development and validation processes that follow. Table 5 summarizes the most important points that should be considered in method development.

Step	Questions, criteria
Choosing the measurement technique	<ul style="list-style-type: none"> <li>• What information do I require?</li> <li>• Which measurement techniques can in principle be used?</li> <li>• How do the different measurement techniques compare with regard to accuracy of results, and robustness and sensitivity of the method?</li> </ul>
Sample preparation	<ul style="list-style-type: none"> <li>• Sample size, sample geometry.</li> <li>• Contact with crucibles (TGA, DSC), clamping assemblies (TMA, DMA).</li> <li>• Thermal pretreatment (1<sup>st</sup> heating run → thermal history of the sample, production process, 2<sup>nd</sup> heating run → characterization of the material).</li> </ul>
Choosing the crucible	<ul style="list-style-type: none"> <li>• DSC: if possible use the light 20-<math>\mu</math>L aluminum crucibles.</li> <li>• TGA: with end temperatures &lt; 600 °C, if possible use the 40-<math>\mu</math>L aluminum crucibles, otherwise the 30-<math>\mu</math>L or 70-<math>\mu</math>L alumina crucibles.</li> <li>• If required: pressure crucibles, crucibles made of special materials (sapphire, platinum) are also available.</li> </ul>
Temperature program	<ul style="list-style-type: none"> <li>• Temperature range - if possible, allow at least 3 minutes before the first event and 3 min after the last.</li> <li>• Heating rate together with other contributory factors determines the sensitivity and temperature resolution. Basic criterion: the temperature distribution in the sample should always be as homogeneous as possible.</li> <li>• If necessary, use a combination of heating, cooling and isothermal segments (recommended especially for DSC).</li> </ul>
Atmosphere	<ul style="list-style-type: none"> <li>• Open crucible, pierced lid, hermetically sealed crucible; overlapping effects can sometimes be separated from one another.</li> <li>• Inert or reactive atmosphere.</li> </ul>
Sample after the measurement	<ul style="list-style-type: none"> <li>• Loss of mass? (offline thermogravimetry)</li> <li>• Morphology?</li> <li>• Color?</li> </ul>
Evaluation	<ul style="list-style-type: none"> <li>• Possibly use a standard method?</li> <li>• Should always be performed according to the same criteria.</li> </ul>
Planning the experiments	<ul style="list-style-type: none"> <li>• Specification of the number of measurements (repeatability).</li> <li>• Order of sample, reference and blank measurements, specification of the reference materials.</li> <li>• Specification of the statistical methods to be used to analyze the different experiments.</li> </ul>

Table 5. Summary of the most important considerations in method development.

# New in our sales program

## STAR<sup>e</sup> V9.00

The functionality of the extremely powerful and comprehensive STAR<sup>e</sup> software has been extended. Two network solutions are now available:

1. Client Server
2. Terminal Server

Both solutions facilitate efficient integrated teamwork in larger user groups. Data is stored in a common database and can be accessed by all users depending on their user rights.

Following a number of customer requests, we have also modified the database concept. Besides the active working database, old archive databases are also available for read-only access.

For data protection reasons, Audit Trail access is protected with a special user right

	Terminal Server	Client Server
<b>Advantage</b>	<ul style="list-style-type: none"> <li>• Requires only one STAR<sup>e</sup> software installation/update</li> <li>• An old PC (thin PC) can be used as a terminal</li> </ul>	<ul style="list-style-type: none"> <li>• Separate installation of the STAR<sup>e</sup> software and database</li> </ul>
<b>Comments</b>	<ul style="list-style-type: none"> <li>• All terminal sessions run on the terminal server. This affects the performance.</li> </ul>	<ul style="list-style-type: none"> <li>• The STAR<sup>e</sup> software must be installed/updated on every client PC</li> <li>• Client PCs are normal PCs</li> </ul>

so that not all users can see who has done what, when and why.

In addition, known errors have been eliminated and smaller improvements made such as:

- Segments with settling (only for the new DSC823<sup>e</sup>)

- Synchronization and triggering of externally connected instruments, for example for photocalorimetry (only for the new DSC823<sup>e</sup>)
- Storage of the Experiment Buffer
- Automatic text export of measured data in ASCII at the end of the experiment

## DSC823<sup>e</sup>

The DSC823<sup>e</sup> replaces the well-known DSC822<sup>e</sup>. The DSC823<sup>e</sup> is currently the most powerful DSC with respect to the two most important DSC characteristics resolution and sensitivity. The DSC823<sup>e</sup> is a basic requirement for using the new TOPEM<sup>®</sup> temperature-modulated technique.



Performance details			
Temperature range		-150 to +500 °C (200 W)	-150 to +700 °C (400 W)
Calorimetric details		<b>FRS5</b>	<b>HSS7</b>
Sensor type		ceramic	ceramic
Number of thermocouples		56	120
Signal time constant		1.7 s	3.9 s
Indium peak		Height to width	17
TAWN	Resolution	0.12	0.30
	Sensitivity	11.9	56.5
Measurement range		at 100 °C	±350 mW
Resolution			±160 mW
Digital resolution			0.04 µW
Sampling rate			0.01 µW
Options	Sample robot	16 million points	
	Gas box	maximum 50 values/second	
	Cooling	34 positions	
	Operation	2 switchable gases	
		Air, cryostat, IntraCooler and liquid nitrogen	
		Automatic furnace lid and LCD-display, switched power supply	

# TOPEM<sup>®</sup> – The new multi-frequency temperature-modulated technique

## Introduction

In a conventional DSC measurement, the heat flow in a sample is measured while the sample is heated or cooled at a constant rate of change of temperature or under isothermal conditions.

The measured heat flow is the sum of the sensible and latent heat flow components. The sensible heat flow component (reversing heat flow) arises from the heat capacity, and the latent heat flow part (non-reversing heat flow) from chemical reactions, crystallization and vaporization processes.

$\phi_{\text{total}}(t) = \phi_{\text{reversing}}(t) + \phi_{\text{non-reversing}}(t)$   
with

$$\phi_{\text{reversing}}(t) = c_p \cdot m \cdot \beta$$

where

- $c_p$  is the specific heat capacity,
- $m$  the mass and
- $\beta$  the heating rate

If the two events occur separately, the interpretation and evaluation of the DSC curve is usually straightforward. With complex processes, where the effects for example overlap, reliable interpretation and evaluation requires measurement techniques that can distinguish between the sensible and latent heat components. Methods based on temperature-modulated DSC (TMDSC) facilitate the separation and provide additional information about the dynamics of the processes involved.

## TMDSC development [1]

The separation of heat flow into sensible and latent parts has been of interest ever since the first thermometric experiments in 1887 by H.L. Le Chatelier and the temperature difference measurements in 1899 by William C. Roberts-Austen.

The first temperature-modulated experiments for the accurate determination of  $c_p$  values can be traced back to the work of O.M. Carbino in 1910. He performed the experiments in a calorimeter.

On the DSC side, the development was not quite so rapid. In 1955 S.L. Boersma intro-

duced the technique of dynamic heat flow calorimetry, making quantitative heat flow measurement possible for the first time.

Scientists like S.C. Mraw and D.F. Naas (1979), H. Dörr (1980) and P.K. Dixon (1990) began to look into the separation of overlapping processes using DSC instrumentation. With the advent of modern computer technology, these techniques became available for an ever-increasing number of users.

METTLER TOLEDO is proud to announce that with the invention of TOPEM<sup>®</sup>, it has achieved another major breakthrough in the field of temperature-modulated DSC, in addition to the well-known IsoStep<sup>®</sup> and ADSC methods.

## Principles of the TOPEM<sup>®</sup> technique

To gain as much sample information as possible from one measurement, a pulse modulation is used that allows the measuring system to be completely character-

In the TOPEM<sup>®</sup> technique, the temperature pulses have a small pulse height and a stochastically (randomly) changing pulse duration (pulse width). Such pulses contain many different frequencies.

The principle of the measurement is shown in Figure 1. The DSC together with the crucible and sample comprise the measurement system to be analyzed. The sample information is derived by correlating the heat flow with the heating rate. A temperature profile and the corresponding heat flow are shown in Figure 2.

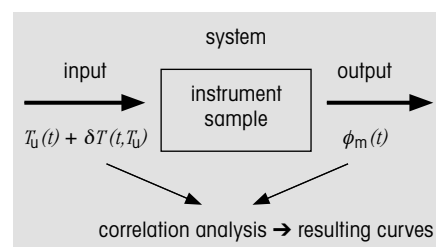


Figure 1. Diagram of the signal flow in a DSC.  $T_u$  is the underlying temperature program ( $T_u = T_0 + \beta_u \cdot t$ , where  $T_0$  is the start temperature and  $\beta_u$  the constant underlying heating rate),  $\delta T$  is the stochastic temperature modulation and  $\phi_m$  the measured heat flow.

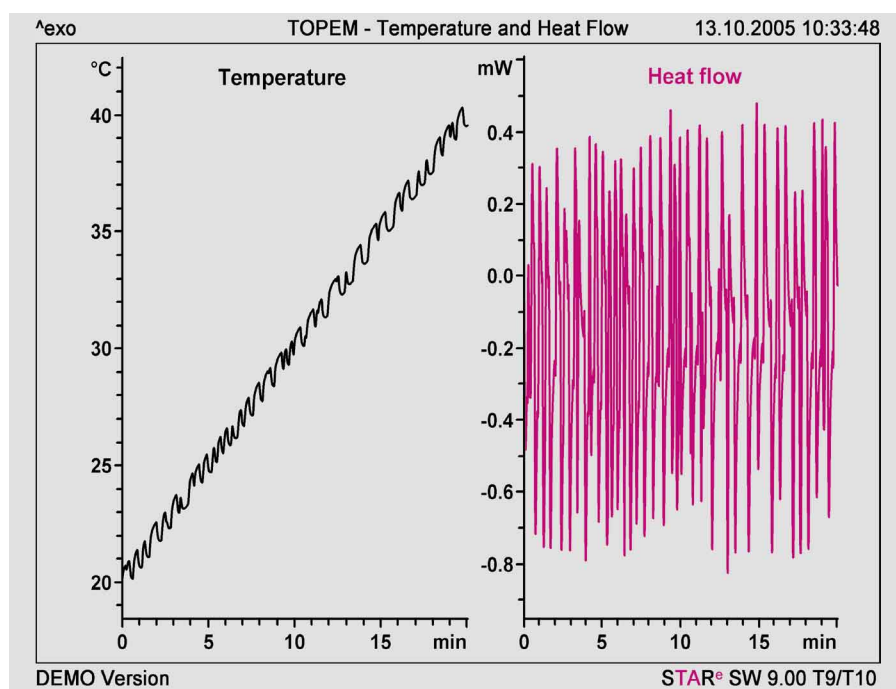


Figure 2. Typical temperature profile and corresponding heat flow in a TOPEM<sup>®</sup> measurement.

TOPEM® allows the dynamics of the system to be analyzed over a broad range of frequencies in one single measurement. The sensible heat flow is based on the quasi-static heat capacity.

## Features and Benefits

**One measurement** – simultaneous determination of sample properties as a function of time and temperature over a wide frequency range

**$c_p$  calculation from the pulse response** – very accurate determination of the quasi-static, specific heat capacity

**Simultaneous high sensitivity and high resolution** – allows the measurement of low energy transitions or close-lying temperature-dependent effects

**Separation of sensible and latent heat flow** – heat capacities can be determined even if the effects overlap

**Simplifies the interpretation of curves** – frequency-dependent effects (e.g. glass transitions) can be easily distinguished from frequency-independent effects (e.g. loss of moisture)

**Extended PEM technique** – eliminates instrumental influences and extends the measurable frequency range

**Automatic  $c_p$  adjustment** – allows the determination of accurate frequency-dependent heat capacity values in one single measurement

## Application example

PET is an excellent example to illustrate the possibilities of the new modulation technique. In a first step the software calculates the following four curves from the modulated heat flow curve:

- Total heat flow
- Sensible heat flow
- Latent heat flow
- Quasi-static, specific heat capacity,  $c_{p0}$

Both the glass transition and the cold crystallization are clearly visible in the modulated heat flow curve. For a more accurate

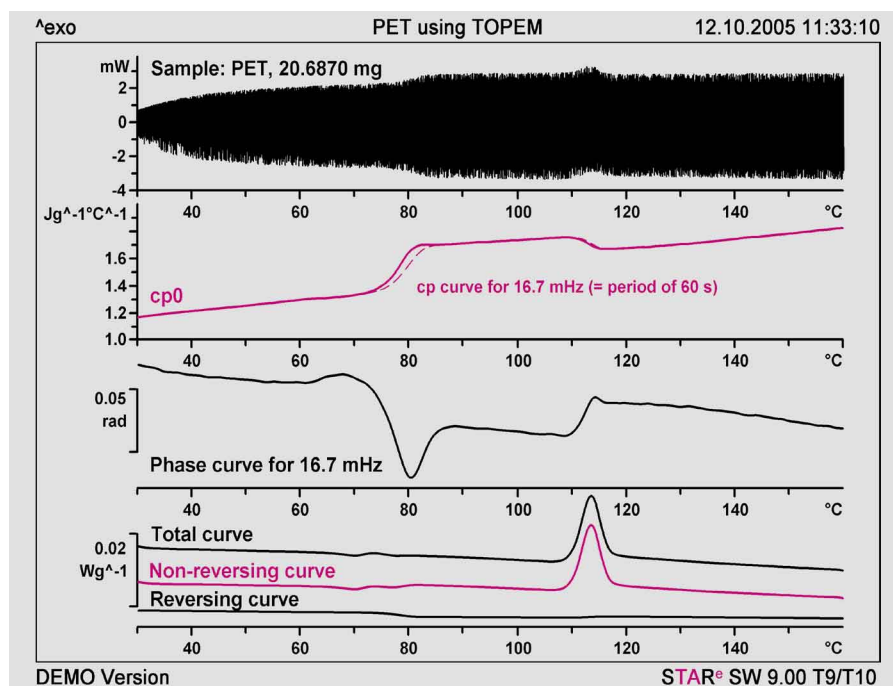


Figure 3. The modulated heat flow curve (above) is compared with the different curves that can be derived from it.

interpretation, however, the calculated individual curves are more useful. During the glass transition at about 80 °C, the heat capacity increases, but decreases again slightly at the cold crystallization. This behavior is even more pronounced in the phase curve. In addition to the quasi-static  $c_{p0}$  curve, the diagram shows a  $c_p$  curve with a measurement frequency of 16.7 mHz. The temperature shift to higher temperatures with increasing frequency at the glass transition can be clearly seen. In contrast, at the cold crystallization, no shift is observed because this effect depends only on the temperature.

## TMDSC method comparison

The three METTLER TOLEDO TMDSC methods differ with respect to the temperature program and the type of evaluation.

### IsoStep®

In IsoStep®, the temperature program consists of small heating steps, followed by isothermal segments.

In general, the duration of each isothermal segment is chosen so that at the end the heat flow remains constant. Quasi-static conditions are thus effectively achieved. For this reason, the measured component of the heat flow corresponds practically to the latent heat flow. The heat capacity is deter-

mined from the heating segments. The advantage of this method is that the measurement is performed quasi-statically, which allows almost complete separation of the latent and sensible heat flows.

### ADSC

In this modulation technique with periodic sinusoidal temperature changes, the “total heat flow” is calculated by signal averaging. It corresponds to the measured curve in a conventional DSC experiment. From the periodic component of the heat flow, one obtains the heat capacity  $c_p(f)$  at the modulation frequency  $f$  chosen for the experiment. In this type of modulation, quasi-static conditions are normally not attained during a thermal event. In this method, the non-reversing heat flow is the difference between the total heat flow and the reversing heat flow.

$$\phi_{\text{non-reversing}}(t) = \phi_{\text{total}}(t) - \phi_{\text{reversing}}(t)$$

The advantage of the method lies in the relatively short measurement time and the possibility of determining the frequency dependence of the heat capacity. Knowledge of the frequency dependence allows information to be obtained about the dynamics of processes. Several measurements at different frequencies are however necessary.

## TOPEM®

This new modulation technique has been patented by METTLER TOLEDO. The results obtained in the two methods described above are now obtained in one single measurement. In a **TOPEM®** measurement, the heat capacity is determined under quasi-static conditions. The separation into sensible and latent heat components is very easy. Frequencies can be selected afterward allowing additional frequency-dependent information to be calculated without the need to perform additional measurements.

## Literature

- [1] Eberhard Gmelin: Classical temperature-modulated calorimetry: A review, *Thermochimica Acta* 304/305 (1977) 1-26

## Summary

Quantity	IsoStep®	ADSC	TOPEM®
Total heat flow (corresponds to the conventional DSC measurement)	No	Yes	Yes
Sensible heat flow	Yes ( $c_{p0}$ based)	Yes ( $c'_{p,fi}$ based)	Yes ( $c_{p0}$ based)
Latent heat flow	Yes	Yes	Yes
Quasi-static $c_{p0}$	Yes	No	Yes
$ c^*_{p,fi} $	No	Yes	Yes, n*
$c'_{p,fi}$	No	1	Yes, n*
$c''_{p,fi}$	No	1	Yes, n*
$\varphi_{fi}$	No	1	Yes, n*
Comments	<ul style="list-style-type: none"><li>• Easy to understand</li><li>• Based on the <math>c_p</math> sapphire standard method</li><li>• Sapphire used as reference</li></ul>	<ul style="list-style-type: none"><li>• Widely used TMDSC method</li><li>• Aluminum used as reference</li></ul>	<ul style="list-style-type: none"><li>• Simultaneous, multi-frequency technique</li><li>• Sapphire used as reference</li></ul>

\* means that for each selected frequency such a curve can be calculated

For further information, see the **TOPEM®** data sheet (ME 51 724 435).

# Applications

## Estimation of the long-term stability of materials using advanced model free kinetics

Dr. Jürgen Schawe

The article describes how advanced model free kinetics can be used to make predictions about the long term-stability of materials, using the decomposition of polystyrene (PS) as an example.

A combination of heating and isothermal measurements as well as an iterative comparison between the predictions of the kinetics and measurement results proved successful.

### Introduction

An important application of model free kinetics is to predict the course of a chemical reaction for conditions under which the reaction can only be measured with difficulty or not at all. To do this the reaction is measured in a readily accessible temperature range and the results used to predict the behavior in another temperature range. The extrapolation of kinetics data

can however only be performed with good accuracy if the reaction mechanism at a conversion,  $\alpha$ , does not change significantly with temperature. This is generally the case for predictions close to the temperature range in which the measurements were performed. However, in the estimation of the long-term stability of materials, the measurements are performed in a relatively high temperature range (e.g.



polymer decomposition at about 300 °C) while the predictions are for room temperature. Care must be taken when making predictions about the kinetics of a reaction over such a large temperature range because reaction mechanisms can change considerably and in particular the changed influence of diffusion processes must be taken into account. A prediction should therefore whenever possible be compared with experimental data, for example from isothermal measurements. Here of course a compromise has to be made between the measurement time available and the observed temperature range. Predictions from kinetics data are more accurate at low measurement temperatures, but the measurement time required and the demands put on the measurement technique are however higher. The advanced model free kinetics software allows data from heating measurements, isothermal measurements as well as from measurements with any temperature segments to be simultaneously included in the calculation. This is why this kinetics software is especially suitable for predicting the long-term behavior of materials.

This article describes a procedure for the prediction of reactions at low temperatures. Thermogravimetric data was used for the evaluation; polystyrene was chosen as model substance.

## Experimental details

The decomposition of polystyrene was measured using a TGA/SDTA851<sup>e</sup>. The samples weighed about 10 mg and were contained in 30- $\mu$ L crucibles; the purge gas was nitrogen. The change in mass of the samples was measured at different heating rates in the range 50 °C to 500 °C or at a constant reaction temperatures. Relatively low heating rates of 1, 2, 5 and 10 K/min were used because predictions for the course of the reaction at low temperatures were required.

The isothermal measurements were performed by inserting the samples into the furnace at 50 °C and heating them to the reaction temperature at different heating rates between 10 and 40 K/min. This temperature program was chosen to ensure that no reaction occurred when the sample

was inserted, and also to allow a reaction that occurred on heating to be taken into account in the kinetics evaluation. If the heating segment employed to reach the isothermal reaction temperature always used the same heating rate, the reaction occurring in this segment would not be adequately taken into account in the kinetics evaluation.

## Procedure for prediction of long-term stability

### Step 1: Consistency test

The first step is to investigate how the kinetics of the reaction differs in heating measurements and under isothermal conditions. This is done by comparing the predictions obtained from the kinetics analysis of the heating measurements with direct measurements. Since this test should be done relatively quickly, ideally a measurement temperature should be used at which the entire reaction is completed within about two hours. This optimum measurement temperature was estimated by first performing the measurements at the higher heating rates (10, 5 and 2 K/min) in order to generate data as quickly as possible. These curves were evaluated while the measurement at 1 K/min was in progress, which is the reason why this curve was not available for the evaluation shown below.

The three curves measured at the higher heating rates were used to calculate conversion curves from which the apparent activation energy curve was then calculated by means of advanced MFK (AMFK). This curve in turn allowed the isothermal course of the reaction to be predicted at a particular temperature. Reaction temperatures between 390 and 350 °C in steps of 10 K and a maximum reaction time of 120 min were chosen. The calculated conversion curves are shown as dashed lines in Figure 1 (right) in the conversion diagram. It can be seen that the reaction is fully completed after two hours at 370 °C. An isothermal measurement temperature of 370 °C was therefore chosen. The sample was heated to this reaction temperature at 30 K/min. The consistency of the AMFK prediction and measurement was checked using only the isothermal segment of the measurement at 370 °C. The corresponding prediction was calculated using the TGA curves measured at 1, 2 and 5 K/min. Figure 2 shows the comparison of the predicted and the measured curves. At a conversion of 50%, the difference in time between the measurement and the prediction was about 5 min. The difference between experiment and prediction indicate that the reaction kinetics changes with temperature. For predicting long-term stability, it follows that the isothermal measurements

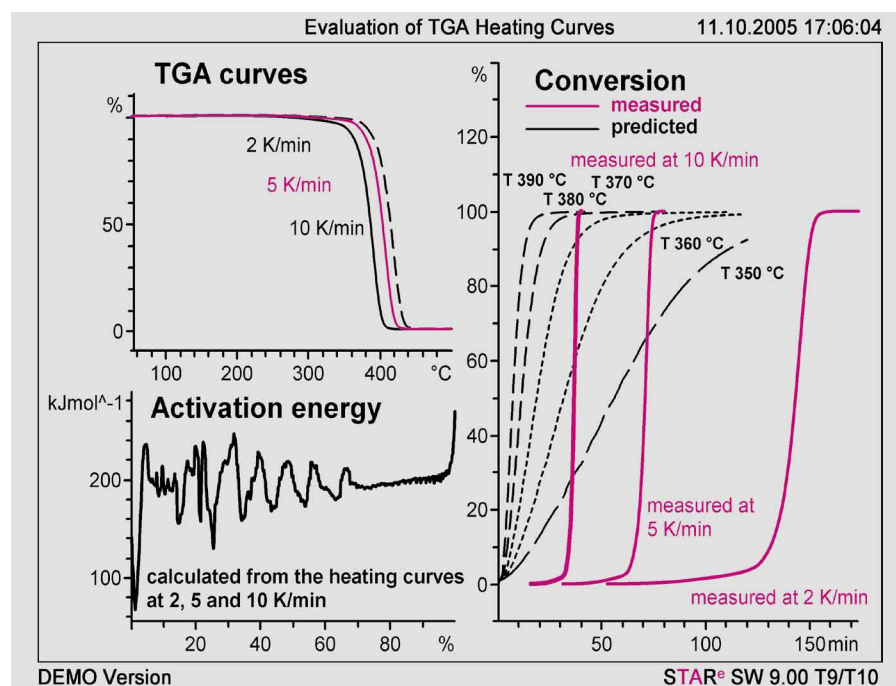


Figure 1. Upper left: TGA curves measured at 2, 5, and 10 K/min. Right: Conversion curves (continuous lines) calculated from the TGA curves and predictions for the isothermal reaction at three different temperatures (dashed lines). Lower left: Calculated apparent activation energy.

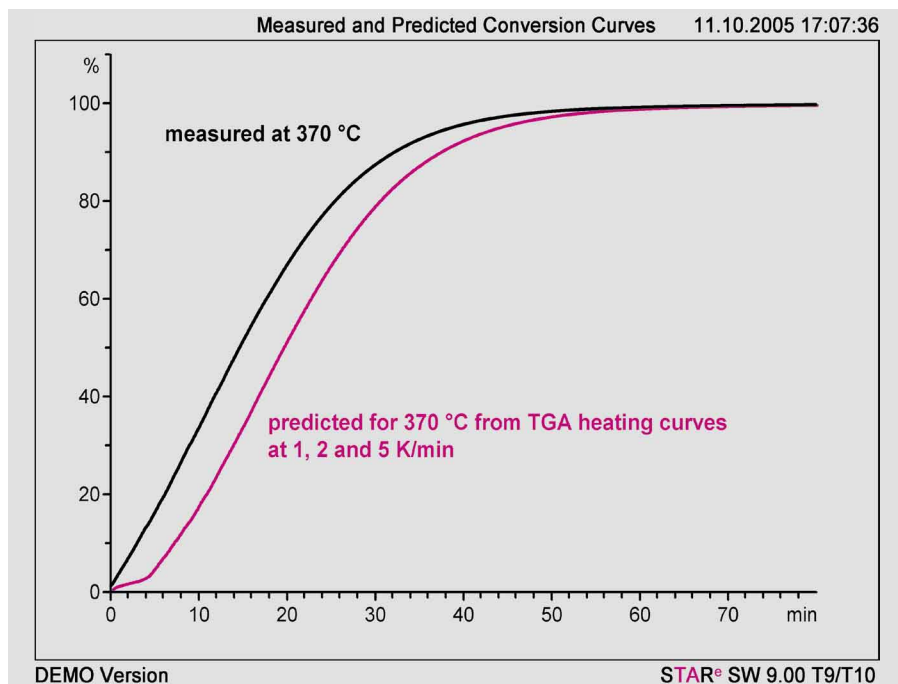


Figure 2. The conversion curve measured at 370 °C and the prediction for the course of the reaction at 370 °C calculated using the different heating measurements.

should be recorded at the lowest possible temperature.

### Step 2: Determination of temperatures for isothermal measurements

For planning further experiments, it is important to decide at which temperatures to perform measurements. Times of 300 min and 500 min were defined for the duration of the isothermal segments. Predictions for isothermal conversion curves were calculated using the activation energy curve calculated from the heating curves recorded at 2 and 1 K/min as well as from the isothermal measurement at 370 °C (including the heating segment). Based on this information, reaction temperatures of 335 °C and 345 °C were chosen. The measurement programs used were:

- Heating from 50 to 345 °C at 20 K/min; then 300 min isothermally at 345 °C
- Heating from 50 to 335 °C at 40 K/min; then 500 min isothermally at 335 °C

Conversion curves were then calculated from the measured curves (including the heating segment). The resulting conversion curves are displayed in the diagram (right) in Figure 3.

A new activation energy curve was then calculated using data from all the conversion curves. For comparison purposes,

another activation energy curve was determined from the isothermal measurements. To compare predictions for the long-term behavior, conversion curves for conversions of 5% and 10% in the temperature range 200 to 300 °C were calculated from both activation energy curves. A small deviation can be seen in the prediction for 5% conversion.

### Step 3: Comparison of predictions with experimental data

The accuracy of the predictions were assessed experimentally. In this case, a measurement temperature of 320 °C was chosen. A prediction for the isothermal course of the reaction at 320 °C was calculated from the activation energy curve (calculated from the isothermal measurements) displayed in Figure 3. This curve shows that at this temperature the measurement time is about 1500 min. The corresponding conversion curve is displayed together with the other isothermally measured curves in Figure 4. The conversion curves for 370 °C, 345 °C and 335 °C were used to calculate an activation energy curve (activation energy curve 1) from which the conversion curve for 320 °C and the iso-conversion curves for 5% and 10% were predicted. A comparison with the measured curve in Figure 4 shows that the course of the conversion curve predicted in this way is slightly slower than that of the direct measurement. If the measured curve of 320 °C is also used to calculate the activation energy curve (activation energy curve 2), then the prediction and measurement agree extremely well. From this it can be concluded that the resulting iso-conversion curves more accurately describe the decomposition of the material. It is quite

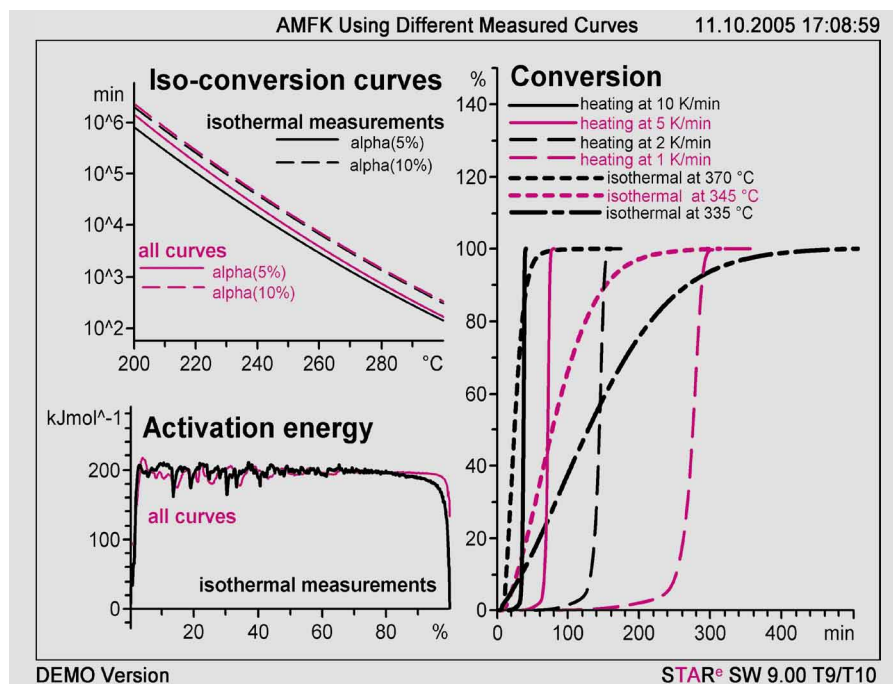


Figure 3. Right: Conversion curves calculated from the heating measurements and the isothermal measurements (including the heating segment). Lower left: Activation energy curves calculated from all measurements (red) and from the isothermal measurements (black). Upper left: Predictions (iso-conversion curves) for conversions of 5% and 10%, calculated from the two activation energy curves.

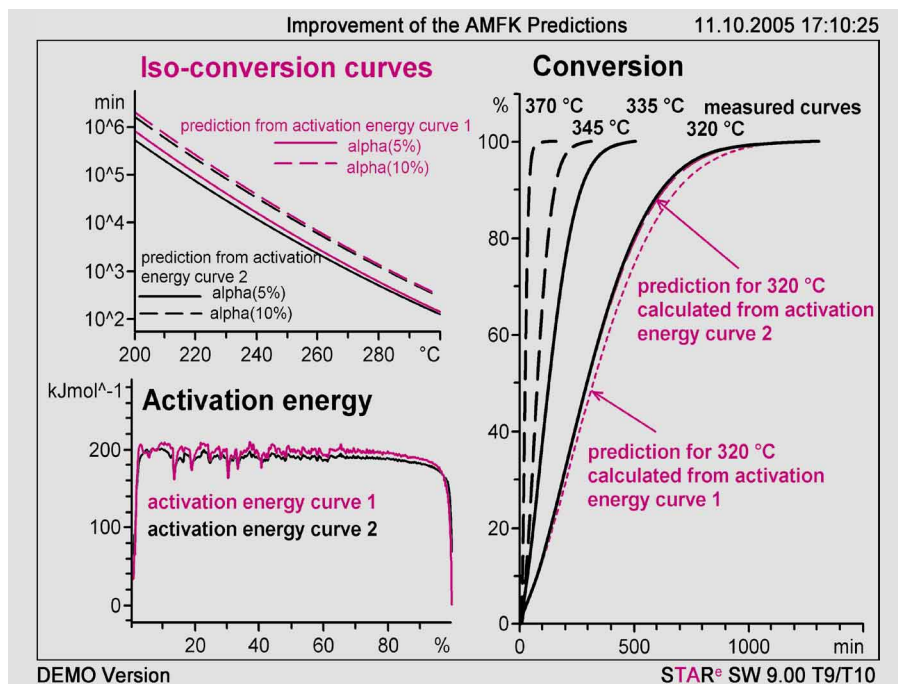


Figure 4. Right: Conversion curves from the isothermal measurements, and two predictions for the isothermal reaction at 320 °C. Lower left: Curves of the activation energy calculated from the measurements at 370 °C, 345 °C and 335 °C (activation energy curve 1) and calculated from all the isothermal measurements (activation energy curve 2). Upper left: Predictions (iso-conversion curves) for 5% and 10% conversion using both activation energy curves.

possible to improve the quality of the prediction by using additional curves measured at lower temperatures for the evaluation. The limitation is however determined by the available measurement time. To accelerate the measurement process, the measurement can be terminated before the reaction has gone to completion. One should however note that predictions cannot be made for conversion values greater than the smallest final value of any of the measured conversion curves. In practice, the minimum measured conversion should be greater than 10%.

## Conclusions

The possibilities offered by advanced MFK are ideal for the iterative improvement of predictions on the course of reactions if one wants to extrapolate over a large temperature range. To do this, the predictions of the kinetics evaluation are first

compared with the isothermal measurements. In a further step, the measured data is then used for the kinetics calculations. This approach allows the predictions of long-term behavior of materials to be

significantly improved. The example discussed in this article is based on thermogravimetric data in which the reaction is measured to completion. For practical applications it is often not always necessary to measure the full course of the reaction. The measurement can be terminated at a conversion greater than 10% in order to reduce measurement time, especially with long measurement times. This must however be taken into account in the calculation of the conversion curves (see box). Furthermore the predictions of the kinetics evaluation are valid only up to the smallest final value of the measured conversion curves.

The approach discussed here can of course also be applied to DSC measurements.

The study of reactions with low reaction rates (such as occur at relatively low temperatures) requires measured data with good resolution for kinetics evaluation and necessitates the use of sensitive measuring instruments. An ultramicro balance is recommended for thermogravimetric measurements. The sensitivity of DSC measurements can be improved by using the HSS7 sensor.

### Tips for operating the STAR<sup>®</sup> software:

Set the Result Mode to "Segment time" (under <Settings>)

Enter the time range and temperature for the calculated conversion curves under <Kinetics><Conversion Parameter Settings>

Enter the time range and conversion of the predictions for iso-conversion curves under <Kinetics><Iso-Conversion Parameter Settings>

Calculation of conversion curves and iso-conversion curves from the activation energy curve under <Kinetics><Applied AMFK>

Calculation of incompletely measured conversion curves using <TGA><Conversion> just by clicking the measured curve; without setting a frame.

# Thermal analysis experiments with fire-retarded polymers

Dr. Samuel Affolter, Interstaatliche Hochschule für Technik, NTB, Buchs, Switzerland

Dr. Manfred Schmid, Materials Science and Technology, EMPA, St. Gallen, Switzerland

## Introduction

Polymer engineering and manufacturing materials consist of organic macromolecules to which a number of functional additives have been added according to the requirements specified for the particular material. Since polymer materials contain carbon and hydrogen, they are usually easily combustible. For safety reasons, high demands are therefore put on fire prevention, depending on the field of application (e.g. building industry, electrical engineering, transport, etc.). These demands cannot be met by the polymer base material itself.

The addition of suitable fire retardants [1], however, allows adequate fire protection properties to be achieved even with easily flammable large-volume plastics such as ABS or polyolefines (PE, PP).

To generate and sustain a fire, three main requirements have to be fulfilled: a source of combustible material, a source of oxygen and a sufficiently high activation energy. Once a fire has started, complex, usually free radical, decomposition processes (pyrolysis and oxidation reactions) occur. As a rule, these are exothermic in nature. From this point of view, fire retardants can exert their effect by

- Producing competing endothermic chemical reactions to consume the exothermic combustion energy. This helps to cool the system
- Interfering with the free radical and oxidative decomposition processes
- Forming a non-flammable, often foam-like crust as a protective layer, e.g. through charring or carbonization, or the formation of inorganic, glassy materials
- Displacing or eliminating (through chemical reaction) surrounding oxygen, or the dilution of mixtures of flammable gases and oxygen

Nowadays, combinations of different chemicals are also used as fire retardants in order to achieve synergetic effects.

A number of standardized methods are used to investigate fire behavior [1]. These include procedures for determining certain characteristics of materials (e.g. the Limited Oxygen Index (LOI) according to ISO 4598 or Cone Calorimetry according to ISO 5660) as well as industry-specific methods (e.g. Bunsen burner test according to UL 94 for electrical engineering). These measurement and test procedures usually give a practical insight into the fire behavior of the materials or components under investigation and are therefore frequently specified in their requirement profiles.

The characterization of a material with regard to fire behavior according to the current standards is more difficult if only a small amount of material is available or if the geometry of the material available is unsuitable. This is usually the case with more detailed investigations of materials and damage. In such situations, thermal analysis is then often very helpful when used together with conventional chemical analytical methods.

## Thermal analysis of fire-retarded polymers

Fire-retarded polymer materials can be investigated by both Differential Scanning Calorimetry (DSC) and Thermogravimetric Analysis (TGA). The method used depends on the composition of the material and the specific information required. Both methods provide data of great value for fire protection studies.

DSC is used to obtain calorimetric data.

Possible applications are the

- Determination of the onset of decomposition in oxygen-containing atmospheres. The decomposition reaction can be exothermic or endothermic depending on the formulation of the material.
- Characterization of energy-consuming (endothermic) decomposition processes of additives, for example the elimination of water from metal hydroxides

TGA, with suitable heating programs and different gas atmospheres, can be used for the

- Determination of the approximate composition of polymer materials (possibly with the aid of other analytical chemical methods)
- Analysis of volatile reaction products, for example water from metal hydroxides or HBr from brominated fire retardants
- Observation of charring or carbonization, or the formation of glassy crusts, in particular of the carbonization behavior of different formulations

Simultaneous differential thermal analysis SDTA (measurement of the temperature difference between the sample and the surroundings) gives a valuable insight into the energy of processes occurring in the TGA (similar to DSC). This is particularly useful for assessing decomposition behavior.

The results of thermoanalytical investigations do not usually allow direct conclusions to be drawn about other fire protective measurement results. They do however provide important information on the nature of materials and often allow simple quality control methods to be developed. Our own experience confirms that thermal analysis can sometimes be more economical and at the same time provide more decisive information than results from elaborate fire protection test procedures.

The following sections describe the specific behavior of individual fire-retardant systems that have been investigated by thermal analysis.

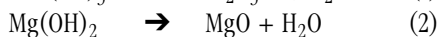
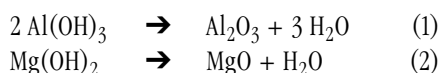
Three typical examples are presented.

1. Aluminum hydroxide in polyolefines, magnesium hydroxide in polyamides
2. Brominated fire retardants in polyethylene
3. Phosphorus in polyamides

The results show how thermoanalytical investigation methods can be used to reproduce particular processes that are directly relevant to fire protection.

## Metal hydroxides

Metal hydroxides such as aluminum hydroxide (and aluminum trihydrate, ATH) or magnesium hydroxide (and magnesium dihydrate, MDH) eliminate water in a fire. The decomposition reaction, eqs (1) and (2), is endothermic and requires between 1000 and 1300 J/g depending on the source of the ATH or MDH. The reaction starts at about 200 °C for ATH, and at about 300 °C for MDH. ATH is therefore often used in materials with processing temperatures below 220 °C, whereas MDH allows temperatures of up to 300 °C to be used.



ATH and MDH used as fire retardants in polymer materials produce a cooling effect due to the water formed on decomposition. The materials often char and carbonize and build a crust together with the metal oxides formed. In addition, the water vapor released dilutes the mixture of combustible gases and oxygen. Metal hydroxides are however only effective at high concentrations (30–60% of the total mass). This can of course have a negative influence on other physical properties of such materials. The processes described can be characterized using thermoanalytical methods. The DSC curves in Figure 1 show the endothermic decomposition processes of pure ATH and MDH. The elimination of water and the low amount of carbon formed can be seen in the TGA measurement of a sample of PE with 50% ATH content (Figure 2).

If the formulation includes only ATH or MDH (besides the polymer), their contents can be determined in three different ways:

- Dehydration energy  $\Delta H$  using DSC
- Mass loss of water by TGA (1<sup>st</sup> decomposition step)
- Ash residue using TGA

Here an absolute uncertainty of measurement  $u_c$  (corresponding to a 99.7% confidence interval) of about 5% is to be expected [3].

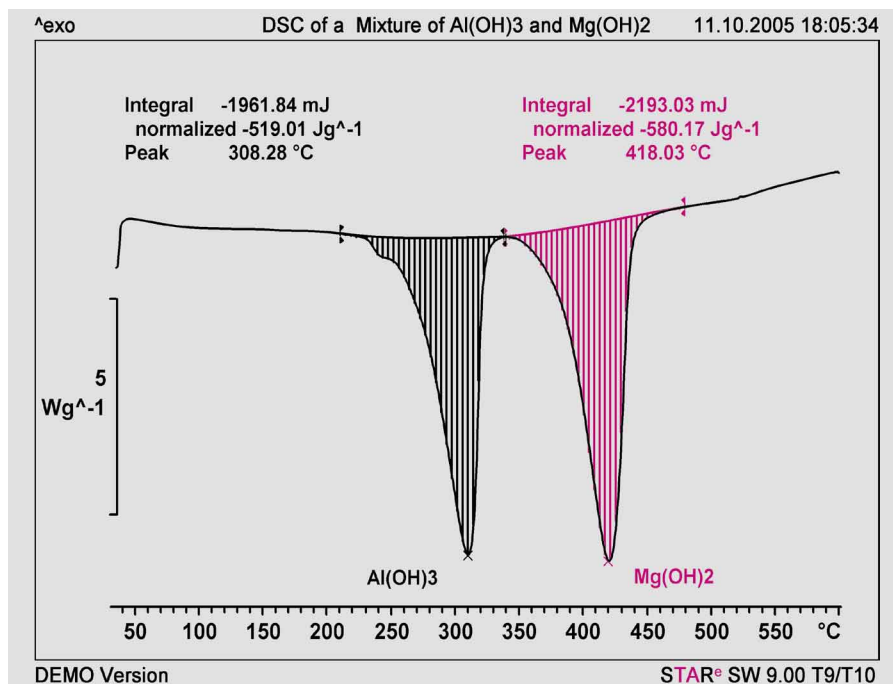


Figure 1. DSC analysis of a 1/1 mixture of ATH and MDH [2] in the range 30–600 °C at 30 K/min under nitrogen.

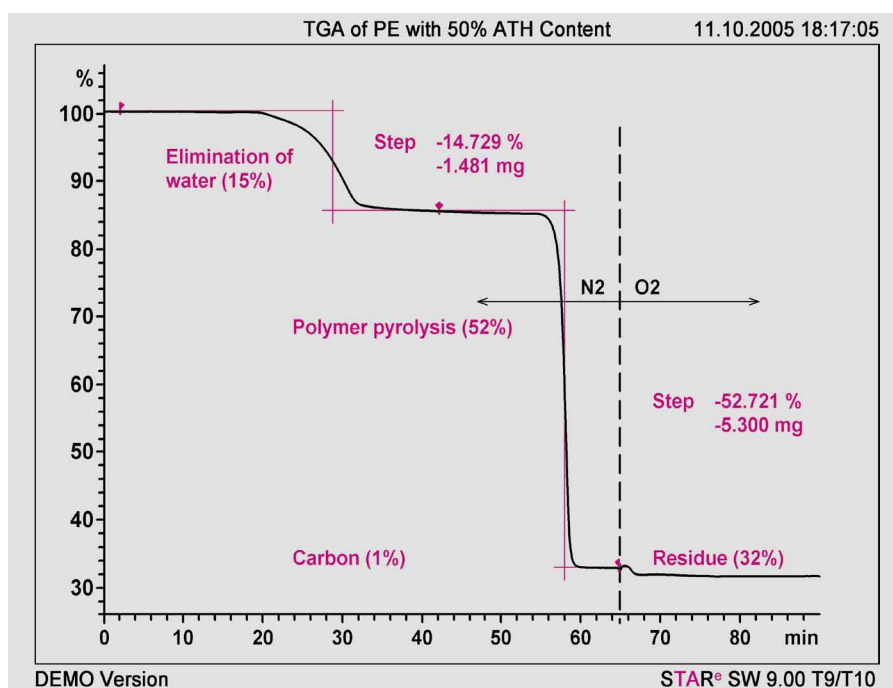


Figure 2. TGA analysis of PE containing 50% ATH [3] – an optimized method for the determination of ATH in polyolefines. TGA program: 30–370 °C at 10 K/min under nitrogen, 20 min isothermal at 370 °C; 370–550 °C at 30 K/min under nitrogen; 550–850 °C at 30 K/min under oxygen.

The determination of ATH and MDH by thermoanalytical methods is however subject to different interferences depending on the formulation of the polymer material [3]. If the ATH or MDH content is determined through the elimination of water, the loss of other volatile substances such as plasticizers or polymer decomposition

products (e.g. acetic acid from ethylene-vinylacetate copolymers, E/VAc) can lead to incorrect results. The determination using the ash residue is made more difficult if thermally inert fillers are present.

For plastics with higher processing temperatures, cheaper naturally occurring min-

erals such as huntite/hydromagnesite are suitable besides the rather costly MDH. Huntite/hydromagnesite eliminates water at about 280-350 °C and carbon dioxide from about 500 °C onward. Both can easily be measured by DSC and TGA [4]. The effectiveness of metal hydroxides in fire prevention can be shown by performing TGA-SDTA experiments in oxygen containing atmospheres. Figure 3 summarizes the investigation of a PA 6 compound containing about 50% MDH. The curves show that the endothermic elimination of water (at about 390 °C) delays the exothermic combustion reaction in comparison to the same measurement of PA 6 without MDH.

### Brominated fire retardants

Brominated fire retardants at concentrations of 10-15% in polymer compounds inhibit free radical chain reactions that take place in the gas phase during combustion. In addition, they form volatile HBr in the presence of hydrocarbons. This helps to dilute the combustion gases. The performance of polymer compounds containing brominated fire retardants is often significantly improved through the synergetic action of antimony trioxide,  $Sb_2O_3$  [1].

Thermal analysis methods can be used to investigate these types of polymer compounds with regard to their fire behavior

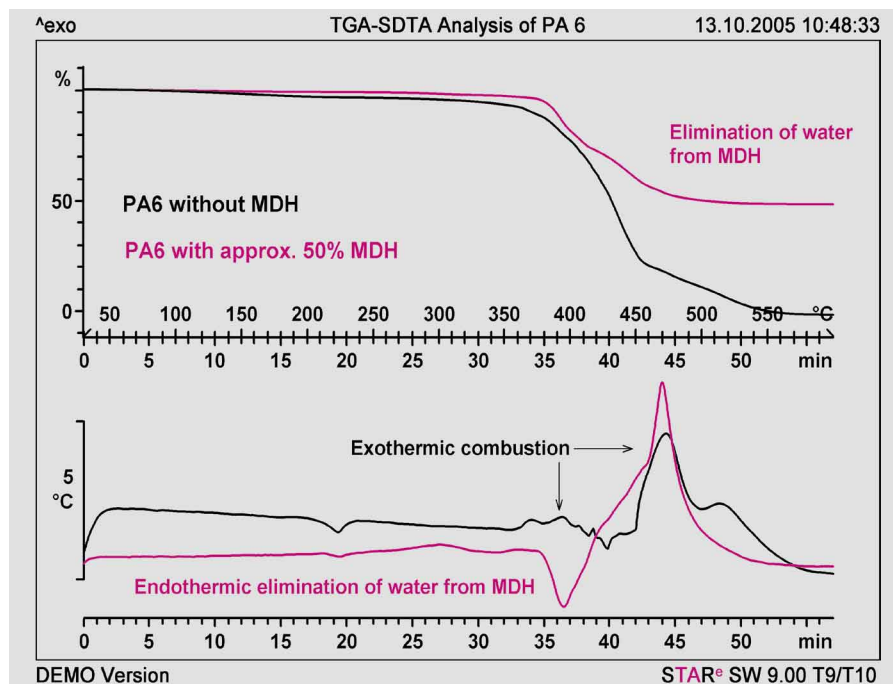


Figure 3. TGA-SDTA analysis of a PA 6 with 10-15% glass fiber and about 50% MDH content compared to a PA 6 without MDH in the range 30-600 °C at 10 K/min under oxygen.

and the corresponding effectiveness of fire retardants. The curves in Figure 4 summarize the decomposition of a PE blend with and without a fire retardant in an oxygen atmosphere. The exothermic combustion reaction is clearly inhibited through the presence of 16% Saytex 8010 (see Figure 5) and 8%  $Sb_2O_3$ . It can also be seen that volatile substances such as HBr are eliminated at about 350 °C, and that the

$Sb_2O_3$  (mp over 650 °C, and bp 1425 °C) reacts to form more-volatile halogenated compounds (e.g.  $SbBr_3$ ) and is therefore no longer present in the ash residue.

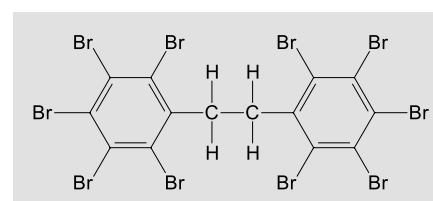


Figure 5. Structure of Saytex 8010; 1,2-bis(pentabromophenyl)-ethane.

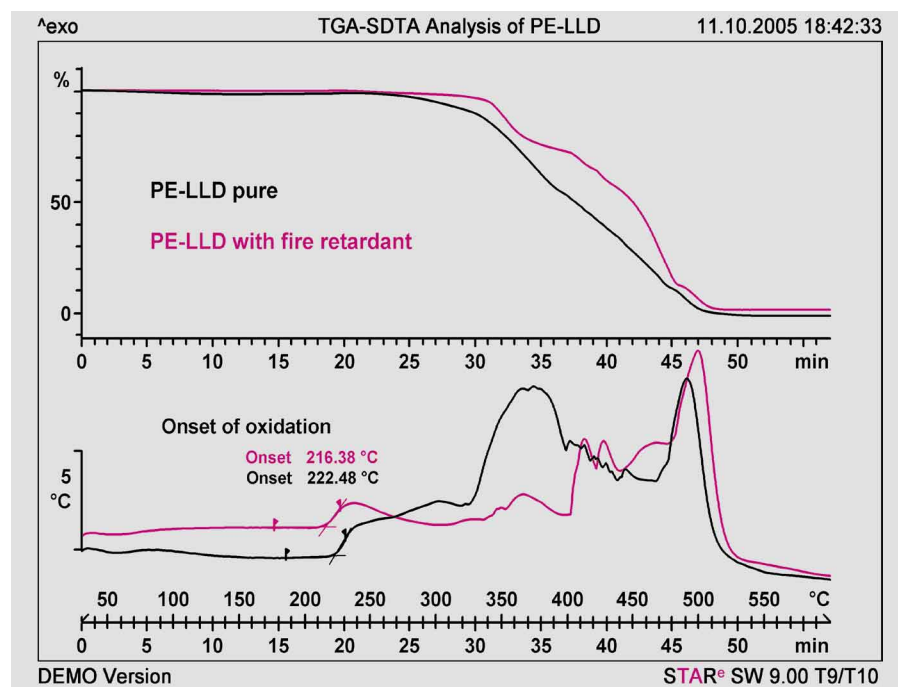


Figure 4. TGA analysis of a PE-LLD sample containing 16% Saytex 8010 and 8%  $Sb_2O_3$ , and a sample of pure PE-LLD in the range 30-600 °C at 10 K/min under oxygen.

However TGA-SDTA and DSC measurements usually provide only rough indications about possible fire behavior. For example, quantitative analyses with TGA are usually impossible because different decomposition processes occur simultaneously and can only seldom be clearly assigned.

Polymer compounds containing brominated fire retardants produce HBr on burning. This forms the strongly corrosive bromic acid in the presence of moisture. Furthermore, trace amounts of poisonous dioxines were detected in fire investigations with many different brominated fire retardants. These two reasons have led to a decrease in the use of such halogenated fire retardants; in some cases their use is even banned by law [5]. The substances are

however very effective fire retardants and in general very compatible with polymers. These properties and their low cost are the main reasons why they are still widely used through the world.

## Phosphorus-containing fire retardants

Elementary red phosphorus finds application particularly with oxygen-containing polymers such as polyamides, PA. The concentration used for PA is normally 7-8% [1]. In a fire, phosphorus exerts its effect mainly in the condensed phase. It reduces the local oxygen content through oxidation and promotes the formation of a non-flammable, carbon-like crust. Furthermore, relatively low quantities of volatile substances are formed and only a small amount of heat is generated [6].

A number of these effects can be investigated by TGA. To illustrate this, two different PA 66 compounds containing glass fiber (25%) were analyzed under different conditions. One of these contained a phosphorus-based fire retardant (7%). The two methods are summarized in Table 1. The main difference between the methods is that in one case the temperature was ramped to 600 °C under nitrogen, and in the other case under oxygen.

### TGA Method 1

Heating ramp: 30-600 °C, 10 K/min, N<sub>2</sub>  
 Heating ramp: 600-850 °C, 30 K/min, O<sub>2</sub>

### TGA Method 2

Heating ramp: 30-600 °C, 10 K/min, O<sub>2</sub>

Table 1. TGA measurement conditions (TGA/SDTA 851<sup>®</sup>).

The measurements obtained with TGA Method 1 under nitrogen are displayed in Figure 6. The curves show that, at higher decomposition temperatures, degradation of the fire-retarded PA 66 (PA-F) is clearly delayed compared with the unprotected PA 66 (PA-N), and that its decomposition takes place in two steps.

Under nitrogen, PA-F hardly shows any carbonization in comparison with PA-N (about 1%). The curves obtained using TGA Method 2 under oxygen (Figure 7) show that significantly smaller amounts of vaporizable or burnable products are

produced and that larger amounts of a carbon-like crust are formed. The decomposition of PA-F begins at a lower temperature than PA-N but leads quickly to the formation of a black product that has not completely burned even at 600 °C: the residue is about 44%.

With a glass fiber content of 25%, this corresponds to about 19% of a newly formed crust-like product. Ashing at 850 °C leads

to the almost complete combustion of these carbon-like products.

Table 2 summarizes the results obtained using Method 2. The results confirm the behavior described at the beginning of this section about polymer compounds that have been fire-retarded with phosphorus.

Similar results have already been described in part in references [6,7].

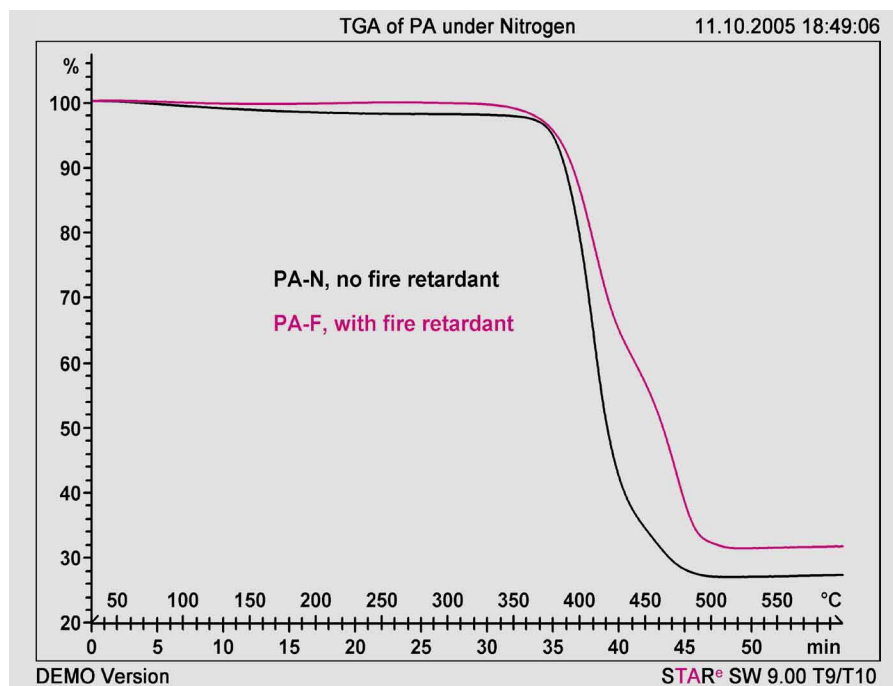


Figure 6. TGA curves of fire-retarded (PA-F) and unprotected (PA-N) PA 66 in the range 30-600 °C at 10 K/min under nitrogen.

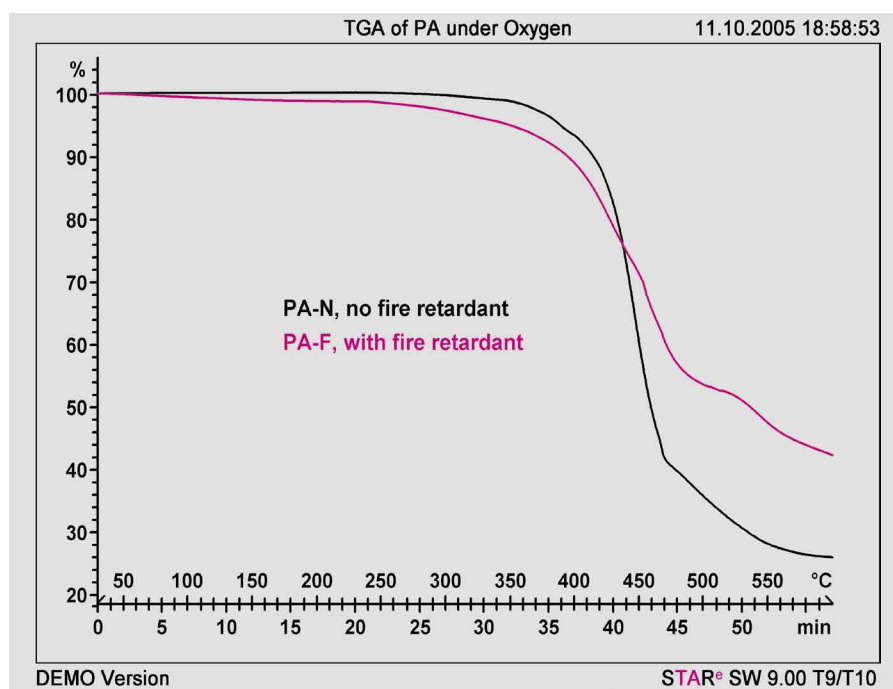


Figure 7. TGA curves of fire-retarded (PA-F) and unprotected (PA-N) PA 66 in the range 30-600 °C at 10 K/min under oxygen.

Name	PA-F	PA-N
Reaction step 1	ab 250-510 °C Loss: 47%	350-470 °C Loss: 58%
Reaction step 2	510-600 °C Loss: 9%	470-600 °C Loss: 16%
Residue at 600 °C	Content: 44% Color: black	Content: 26% Color: white
Ash at 850 °C	Content: 29% Color: almost white	Content: 26% Color: white

Table 2. Decomposition behavior of PA 66 compounds using TGA Method 2 in the range 30-600 °C at 10 K/min under oxygen.

## Conclusions

The results presented here show that thermoanalytical methods such as TGA and DSC can be used to obtain important information about the mechanisms and the effect of fire retardants in polymer materials. This is in particular useful for material development.

To date no investigations have been reported that allow a direct correlation of thermoanalytical data with fire-prevention tests or real fire behavior to be made.

It is very difficult to establish such correlations because realistic fire conditions

cannot be simulated in thermoanalytical experiments using just a few milligrams of sample!

Acknowledgements: The author wishes to thank Huber + Suhner AG, Pfäffikon, Switzerland and in particular Dr. R. Koeppel and his team (Material Development, Wire & Cable Division) for preparing some of the compounds used in this investigation.

## Literature

- [1] P.F. Ranken, 12. Flame Retardants, in H. Zweifel (Editor), *Plastics Additives*

- Handbook, Carl Hanser Verlag, München, 5<sup>th</sup> Edition (2001), p. 681-698
- [2] J.E.K. Schawe, *Collected Applications Thermal Analysis, Elastomers*, Mettler-Toledo Analytical, Vol 2 (2002), p. 153-159
- [3] S. Affolter, M. Schmid, A. Ritter, *Ringversuche an polymeren Werkstoffen 2004*, EMPA St. Gallen and NTB Buchs (2004); Publikation in Vorbereitung.
- [4] G.N. Georiades, B.J. Larsson, C.Pust, *Huntite-hydromagnesite production and applications*, Konferenz-Einzelbericht in *IM Ind. Minerals*, 12<sup>th</sup> Ind. Minerals Internat. Congress, Worcester Park (1996), p. 57-60
- [5] *RoHS-Richtlinie (Richtlinie 2002/95/EG vom 27. Januar 2003 zur Beschränkung der Verwendung bestimmter gefährlicher Stoffe in Elektro- und Elektronikgeräten) WEEE-Richtlinie (Richtlinie 2002/96/EG des Europäischen Parlaments und des Rates vom 27. Januar 2003 über Elektro- und Elektronik-Altgeräte)*
- [6] B. Schartel, R. Kunze, D. Neubert, *Red Phosphorus-controlled Decomposition for Fire Retardant PA 66*, *J. Appl. Polymer Sci.*, 83 (2002), Heft 10, p. 2060-2071
- [7] I.A. Abu Isa, S.W. Jodeh, *Thermal properties of automotive polymers III, thermal characteristics and flammability of fire retardant polymers*, *Mat. Res. Innovat.*, 4 (2001), Heft 2/3, p. 135-143

# The separation of sensible and latent heat flow using **TOPEM**<sup>®</sup>

Dr. Jürgen Schawe

**TOPEM**<sup>®</sup> is a new temperature-modulated DSC technique. Latent and sensible heat flows can be separated and the frequency-dependent heat capacity determined in one single measurement.

## Introduction

In **TOPEM**<sup>®</sup>, a temperature program is used in which an underlying temperature ramp or an isothermal segment is modulated with a series of small temperature pulses of random pulse width. Using this technique, it is possible to separate sensible and latent heat flows from one another.

In addition, the frequency-dependent heat capacity can be determined, which allows conclusions to be drawn about the dynamics of processes.

In this article, we will present several applications that demonstrate the power of this new technique.

## Sensible and latent heat flow

In a DSC experiment, heat is continuously exchanged between the sample and the measuring instrument. If heat is supplied to the sample, its temperature increases, and conversely if heat is removed, its tem-

perature decreases. The term sensible relates to the part of the heat exchanged between the measuring instrument and the sample that results in a change in temperature of the sample. After the supply or removal of heat, the temperature change takes place either immediately or, due to dynamic processes in the sample, after a certain time delay.

If the total sensible heat is to be measured, it follows that a sufficiently long period of time must elapse after the heat has been supplied or removed. In other words, measurement of sensible heat is only possible



under quasi-static conditions. An important characteristic feature of sensible heat is that the processes associated with the uptake or loss of heat can be reversed. Thermodynamically we are dealing with reversible processes that occur close to a local metastable state.

Examples are

- Temperature change outside a thermal event
- Heat capacity changes in second order phase transitions
- Heat capacity changes during chemical reactions
- Glass transitions
- Reversible melting (e.g. of polymers)

The latent heat is the non-sensible part of the total heat flow. It can be endothermic or exothermic and is associated with irreversible changes in structure.

Such processes begin in a thermodynamically non-equilibrium state and end in a (metastable) equilibrium state. They can take place time-dependently or be kinetically controlled and therefore be time dependent.

Examples are:

- Non-reversible chemical reactions
- Crystallization in supercooled liquids
- Melting with supercooled crystallization
- Vaporization of volatile components.

A conventional DSC measurement always measures the sum of the latent and sensible heat. Temperature-modulated DSC (TMDSC) attempts to separate the total heat flow into a sensible heat flow component (often called reversing) and a latent heat flow component (often called non-reversing). If the reversing heat flow is measured dynamically, it is in general less than the sensible heat flow because all time-dependent processes that take longer than the characteristic measuring time (e.g. 60 s) are not measured. In quasi-static measurements, the difference between the sensible and reversing heat becomes minimal. For this reason, using **TOPEM**<sup>®</sup>, it is possible to obtain an excellent separation of sensible and latent heat flows.

## Applications

### Second order transitions

In second order phase transitions, the heat capacity first increases up to a critical temperature and then decreases suddenly. It is a phenomenon in which effects due to latent heat do not occur. Correspondingly no measurement effects are to be expected in the non-reversing heat flow curve.

The solid-solid transition of sodium nitrate at 275 °C was measured as an example. Since the heat capacity change following the critical temperature is expected to take place over a very small temperature range (about 0.1 K), a measurement can only be successful if it is performed at a very low heating rate using a very small temperature modulation. In this case an underlying heating rate of 20 mK/min and a pulse height of 5 mK were used.

The resulting heat flow curves are presented in Figure 1. As expected only the reversing and total heat flow curves show a transition peak. The non-reversing heat flow curve does not show any effect despite the sharp change after the critical temperature. This proves that **TOPEM**<sup>®</sup> is clearly able to differentiate between effects that exhibit sensible and latent heat flows.

### Change in the heat capacity during an isothermal chemical reaction

In a chemical reaction, a change in heat capacity can occur for several reasons:

- Difference in the heat capacities of starting materials and reaction products
- Phase separations
- Vaporization of volatile reaction participants
- Vitrification

In polymerization reactions, the glass transition temperature of the reaction products increases with increasing degree of polymerization. If the glass transition temperature of the reaction product is greater than the reaction temperature, vitrification can occur during the reaction. The viscosity of the reaction mixture then increases markedly and the reaction practically stops. Vitrification is observed as a step in the heat capacity (sensible heat flow) curve. In conventional DSC this step is overlapped by the contribution from the reaction enthalpy (latent heat flow). **TOPEM**<sup>®</sup> allows these two heat flows to be separated from one another. In addition, frequency analysis provides an insight into the nature of the heat capacity change.

If a chemical reaction is performed under quasi-isothermal reaction conditions (i.e. an underlying heating rate of 0 K/min)

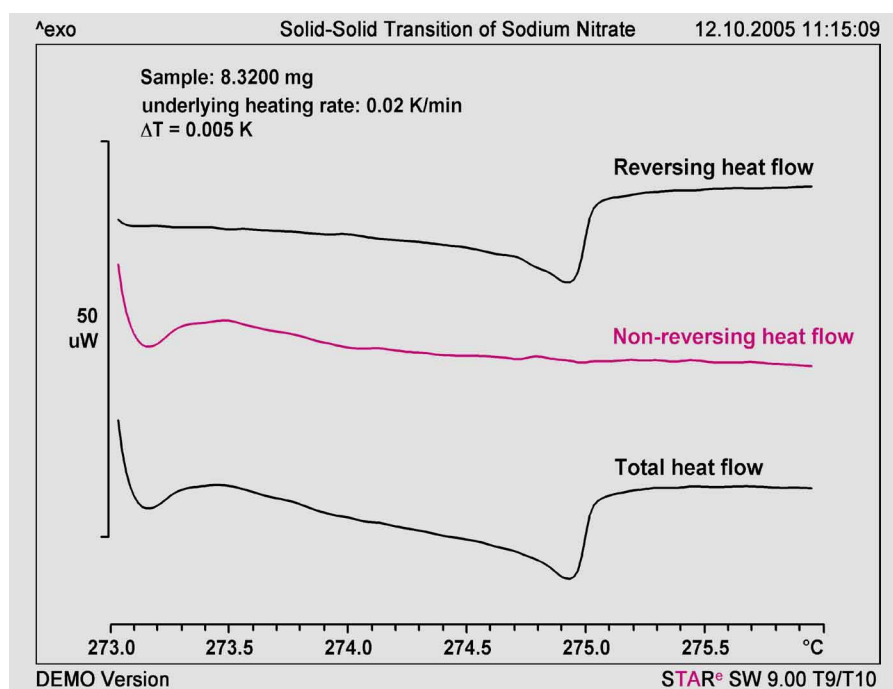


Figure 1. Total, reversing and non-reversing heat flow curves of the solid-solid transition of sodium nitrate at 275 °C.

there can be no reversing heat flow and the total heat flow and the non-reversing heat flow are identical. With **TOPEM**<sup>®</sup>, the quasi-static heat capacity can be measured even under these conditions.

This is illustrated in Figure 2 using a two-component stoichiometric epoxy-amine mixture consisting of the diglycidylether of bisphenol A (DGEBA) and diaminodiphenylmethane (DDM) as curing or cross-linking agent. The reaction was performed at 80 °C.

The total heat flow (in this example, it is identical to the latent heat flow) shows that the reaction peak maximum occurs after about 30 min. Due to the cross-linking reaction, the quasi-static heat capacity of the material first increases. After about 65 min it decreases stepwise (step midpoint is at about 85 min, the vitrification time). The step is due to vitrification: before this step the material is a liquid, and afterward a glassy solid. The frequency-dependent complex heat capacity can also be determined using **TOPEM**<sup>®</sup>. The curves for various frequencies between 17 and 170 mHz are shown in the upper diagram (Figure 2). They show that the vitrification time is shorter at higher frequency. This behavior is characteristic for relaxation processes, in this case, a chemically induced glass transition.

All this information is obtained from just one single **TOPEM**<sup>®</sup> measurement. The measurement of the frequency-dependence of the heat capacity of reactive materials using several sinusoidal modulated TMDSC measurements is often problematical because the reaction kinetics of the individual samples can differ slightly.

### Identification of melting processes

In particular with multicomponent systems or semicrystalline polymers, thermal events can occur that cannot be clearly identified using conventional DSC. This is the case if broad melting processes occur after steps in the heat flow curve (characteristic for glass transitions). It is then often not possible to identify the step with certainty as a glass transition, as the beginning of the melting process, or as a combination of the two processes. In this sort of problem, a

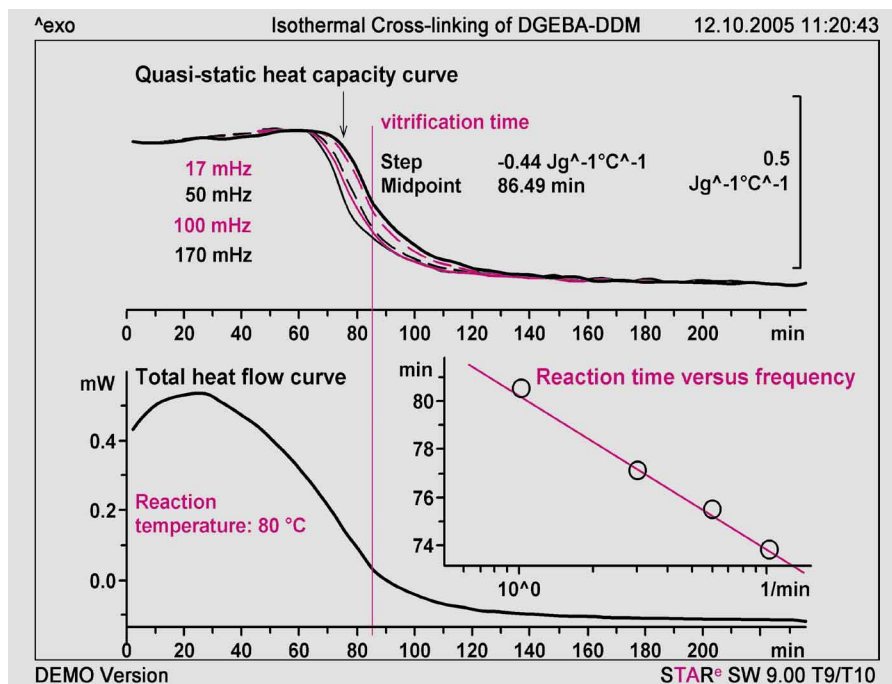


Figure 2. Heat capacity and total heat flow measured during the isothermal cross-linking of a DGEBA-DDM mixture at 80 °C. The inserted diagram shows the frequency dependence of the vitrification process.

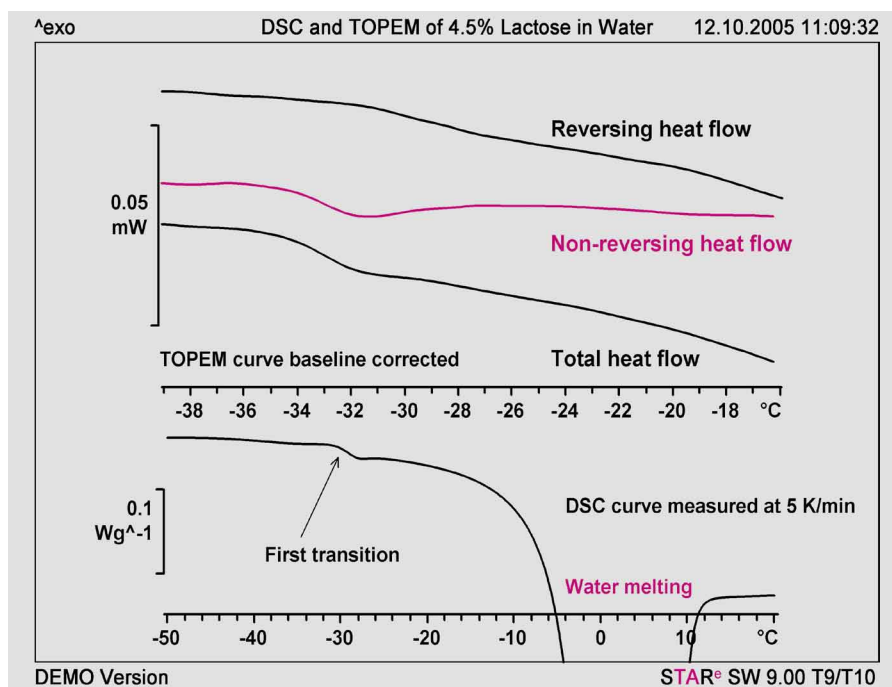


Figure 3. In the lower coordinate system the DSC curve is shown on an expanded ordinate scale and the heat flow step is marked with an arrow. The upper coordinate system shows the results obtained using **TOPEM**<sup>®</sup>.

complete separation of sensible and latent heat is of great help because melting processes are associated with latent heat, whereas glass transitions are apparent in the sensible heat flow.

An example of such a system is a sugar/water mixture. If a mixture with a low concentration of sugar is first slowly cooled, a

small step is observed before the melting peak of water when the sample is heated. This behavior is demonstrated using a water-lactose mixture containing 4.5% lactose (mass percent) in Figure 3. The step mentioned above can be seen at about -30 °C in the DSC curve (labeled “First transition”). In the literature the origin

of this peak has been the subject of much controversy. Using **TOPEM**<sup>®</sup> under suitable measurement conditions, it is possible to clearly distinguish between sensitive and latent heat flows. In this case the measurement was performed at an underlying heating rate of 0.1 K/min and a pulse height for the temperature modulation of 5 mK.

The results are presented in Figure 3. An endothermic peak is clearly visible in the non-reversing heat flow curve. The revers-

ing heat flow curve, however, shows no relevant change. The step-like change of the total heat flow can only be interpreted as the beginning of the melting of water in an amorphous lactose-water environment.

### Conclusions

**TOPEM**<sup>®</sup> is a new temperature-modulated DSC technique in which the linear underlying temperature program is overlaid with a stochastic (random) temperature modulation. This technique makes it possible to

separate latent and sensible heat flow components with a high degree of accuracy. This is extremely helpful, especially for the interpretation of thermal events. The frequency evaluation furthermore allows the complex (frequency-dependent) heat capacity to be determined over a broad frequency range from one single measurement. The information obtained can be used to interpret thermal events as well as for the investigation of the dynamics of processes.

## Tips and hints

# Simple determination of the thermal conductivity of polymers by DSC

Dr. Rudolf Riesen

Simple DSC measurements can be used to rapidly determine the thermal conductivity of polymers and other materials with similarly low values with an accuracy of about  $\pm 10$  to  $\pm 20\%$ .

A procedure for doing this was published in 1985 by Hakvoort and van Reijen. In this method, the melting behavior of a pure metal on top of a cylindrical sample or disk is measured.

To simplify sample handling, we have modified the method by containing the metal in a crucible. The thermal conductivities of 11 polymers were measured and the results compared with literature values. The values we obtained were on average about 4% lower than literature values. This deviation is small if you take into account the general measurement uncertainties associated with thermal conductivity measurements.

### Introduction

Hakvoort and van Reijen [1] proposed an interesting method to determine the thermal conductivity of solid materials. This consisted of putting a pure metal (e.g. indium or gallium) on the upper circular end surface of a sample in the shape of a right circular cylinder or disk, and then placing the disk (without a crucible) directly on the DSC measuring sensor. During heating, the metal reaches its melting point and the temperature remains constant while the metal melts. The temperature of the upper end surface of the disk is thus known at this instant. The temperature of the lower end surface of the disk and the heat flowing into the disk are measured by the DSC. The thermal conductivity of the sample can then be calculated from the temperature difference between upper

and lower end surfaces of the disk and the heat flow.

Besides DSC, many instruments are nowadays available that have been specially designed to determine thermal conductivity. The advantage of DSC, however, is that the specific heat capacity can also be measured with the same instrument. This allows the thermal diffusivity ( $\lambda/(\rho c_p)$ ) of a material to be determined. The method outlined above using the metals has recently been reintroduced to determine the properties of composite materials [2] and new materials [3].

In the following article we will describe a simple DSC method that allows the thermal conductivity of polymers to be rapidly determined typically with a measurement uncertainty of 10%.

## Theoretical background

Under stationary conditions, the heat flow,  $\phi$ , through a body with a thermal resistance,  $R_s$ , is proportional to the temperature difference,  $\Delta T$ :

$$\phi = \frac{1}{R_s} \Delta T \quad (1)$$

The thermal resistance,  $R_s$ , of the material is given by the material-dependent thermal conductivity and the geometry of the body:

$$R_s = \frac{h}{\lambda A} \quad (2)$$

Here  $\lambda$  is the thermal conductivity,  $A$  the cross-sectional area, and  $h$  the length of the body.

With cylindrical samples of diameter,  $D$ , and height,  $h$ ,

$$A = \frac{\pi \cdot D^2}{4} \quad (3)$$

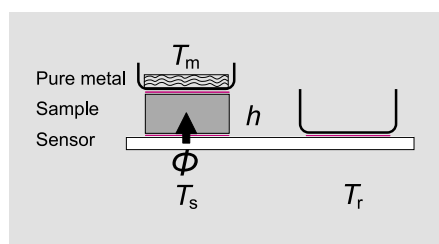


Figure 1. Schematic diagram of the sample arrangement on the DSC sensor.  $h$ : is the height of the sample cylinder;  $\phi$  the heat flow that flows from the sensor into the sample;  $T_m$  the temperature of the metal melt,  $T_s$  the sensor temperature under the sample;  $T_r$  the temperature of the reference sample.

The reference crucible is empty. A crucible of the same type containing the pure metal is placed on the sample. The spaces between the crucible-sample and sample-sensor interfaces are filled with heat transfer oil (red lines).

Figure 1 shows the setup used to determine the thermal conductivity of a material by DSC. The heat flow from the sensor to the pure metal depends not only on the thermal resistance of the sample, but also on the thermal resistances at the sensor-sample ( $R_1$ ) and sample-metal ( $R_2$ ) interfaces. Equation (1) must therefore be rewritten as follows:

$$\phi = \frac{(T_s - T_m)}{R_1 + R_s + R_2} \quad (4)$$

To ensure that the thermal resistances  $R_1$  and  $R_2$  were reproducible, the spaces at the interfaces were filled with heat transfer oil.

It can therefore be assumed that  $R_1$  and  $R_2$  are independent of the sample if the same sample cross-section is always used.

$$R_T = R_1 + R_2 \quad (5)$$

$R_s$  and hence the thermal conductivity of the sample can only be determined if  $\phi$ ,  $R_T$ ,  $T_m$  and  $T_s$  in eqs 4 and 5 are known. The value of  $T_m$  during melting is known because a pure metal is used. The values of  $\phi$  and  $T_s$  are obtained from the DSC measurement, and  $R_T$  can be determined by performing several measurements. If  $R_T$  is much smaller than  $R_s$ , then  $R_T$  can even be neglected and  $\lambda$  can be determined from a single melting curve.

Combining eqs 1 and 2 gives eq 6:

$$\lambda = \frac{\phi}{\Delta T} \frac{h}{A} \quad (6)$$

Equation 6 is valid only during melting.  $\Delta T$  is then the difference between the temperature  $T_s$  at a time  $t$  and the melting point of the metal (i.e. the temperature of the beginning of melting,  $T_{onset}$ ). The corresponding heat flow  $\phi$  is the difference between the heat flow at the same time  $t$  and the heat flow at the beginning of melting (see Figure 2).

$$\frac{\phi}{\Delta T} = \frac{\phi_t - \phi_{onset}}{T_t - T_{onset}} = S \quad (7)$$

$S$  is therefore the slope of the linear side of the melting peak.

Rearrangement of eqs 4 to 7 yields eq 8:

$$\frac{1}{S} = R_T + \frac{h}{\lambda A} \quad (8)$$

If two samples of the same material but with different cylinder heights are measured,  $\lambda$  can be calculated according to eq 9.

$$\lambda = \frac{\Delta h}{A \left( \frac{1}{S_2} - \frac{1}{S_1} \right)} \quad (9)$$

where  $\Delta h$  is the difference of the cylinder heights ( $h_2 - h_1$ ),  $S_1$  is the slope of the DSC curve of the small sample, and  $S_2$  the slope of the DSC curve of the large sample.

If several samples of different heights are used, the thermal conductivity and  $R_T$  can be determined from linear regression of  $1/S$  and  $h/A$ , according to eq 8 [3].

## Experimental details

Pure gallium (29.8 °C) is ideal for measuring thermal conductivity close to room temperature. The gallium sample has to be cooled down to at least 10 °C for it to crystallize. Our measurements were performed using a DSC822<sup>e</sup> equipped with an IntraCooler.

Other temperatures require different metals (e.g. indium). In some cases, it might be possible to use very pure organic substances. However, they must not sublime, must not exhibit polymorphism, and must melt and crystallize reproducibly when used several times.

### Crucible preparation

Hakvoort and van Reijen placed the pure metal directly on the sample disk. To simplify sample handling, we enclosed the metal in a 20- $\mu$ L light aluminum crucible without a lid (Figure 1). Since gallium readily reacts with aluminum, the inside surface of the crucible was coated with a thin film of lacquer (10 to 30  $\mu$ m). This was done by completely filling the crucible with a solution of a clear lacquer in a suitable solvent (about 10-fold dilution). We used so-called "Nitrohartgrund" (a nitrocellulose wood primer) and nitro thinner. The solvent was evaporated by slowly heating to 80 °C and the amount of resin remaining in the crucible determined by back-weighing. Afterward, sufficient pure gallium (about 80 mg) was weighed into the crucible so that the bottom of the crucible was completely covered when the gallium melted. The crucible can be used several times. It is advisable to periodically check whether the melting enthalpy and melting temperature remain constant. Any change in the values would indicate alloy formation (a possible second peak) and/or oxidation.

### Polymer samples

A number of different polymers and materials available in the form of films or sheets were chosen as test materials for our studies. Disks with a height of 0.5 to 1.5 mm were punched out from these materials. The circular end surfaces were carefully polished with fine emery paper so that the height could be accurately determined to at least 10  $\mu$ m and the diameter to 20  $\mu$ m. The diameter of the samples was the same

Polymer		Literature value	Selected comparison value	Comments
		Wm <sup>-1</sup> K <sup>-1</sup>	Wm <sup>-1</sup> K <sup>-1</sup>	
Cork		0.07	0.07	
Polystyrene	PS	0.13 to 0.16	0.16	
Polyvinylchloride	PVC	0.15 to 0.21	0.16	
Acrylonitrile-butadiene-styrene	ABS	0.16 to 0.18	0.17	
Polypropylene	PP	0.12 to 0.22	0.17	
Polymethylmethacrylate	PMMA	0.10 to 0.20	0.20	
Polyamide	PA 66	0.23 to 0.33	0.24	Moisture influence
Polytetrafluorethylene	PTFE	0.25 to 0.26	0.25	
Polyethylene terephthalate	PET	0.15 to 0.29	0.27	Crystallinity
Polyethylene low density	PE	0.32 to 0.48	0.32	Density 0.914
Phenol-formaldehyde thermoset	PF	0.3	0.30	

Table 1. Samples and literature values of the thermal conductivity (data from different sources according to the literature list).

as that of the bottom of the crucible (6 mm). Table 1 shows the materials used with the literature values for their thermal conductivities.

Some literature values vary markedly. A possible reason for this is that the thermal conductivity of polymers also depends on their degree of crystallinity, density, moisture content, filler content and the presence of other additives. Table 1 therefore lists the range of values found and the comparison value chosen for the measurements. Many authors quote accuracies of plus or minus a few percent for their  $\lambda$  values. However, the large scatter in the literature values shows that one must reckon with greater measurement uncertainty when determining thermal conductivity.

### Sample preparation and measurement method

To achieve the best possible reproducibility for the thermal resistances, the spaces at the crucible-sample and sample-sensor interfaces were filled with the minimum amount of a heat transfer oil to provide complete contact between the surfaces. First, oil was applied to the upper face of the sample and the crucible placed on top of it. This essentially fixed the crucible in place and allowed it to be precisely oriented.

A very small amount of oil was then applied to the lower face of the sample. The sample with the crucible on top was then carefully placed on the sensor. An empty crucible was used on the reference side.

The temperature gradients over the sample were kept small by using a low heating rate (0.5 K/min). The purpose of this is to minimize

the possibility of alternative routes for heat flow (that would escape measurement). The following temperature program was used: Heating from 28 to 38 °C at 0.5 K/min, followed by cooling to -5 °C at 10 K/min to ensure that the gallium solidified again after the measurement. Purge gas: nitrogen 50 mL/min to prevent oxidation of the gallium.

### Evaluation

The slope,  $S$ , is determined by plotting the DSC curve against sample temperature ( $T_s$ ) (see Figure 2, red coordinates). The curve of the sample temperature is also displayed (black coordinates, but is not used in the calculation). When determining the onset temperature, you must make sure that the tangents lie exactly on the DSC curve. The slope  $S$  of the second tangent can be read off directly in the result block.

### Results

Table 2 summarizes the measured thermal conductivities. The results in column “ $\lambda$  Direct” were determined using eq 6 with just one measurement each time. The values in the column “ $\lambda$  Difference” were calculated using eq 9. Here, for simplicity, the slope of the melting peak without sample (only crucible,  $S_1 = 90 \text{ mW}\cdot\text{K}^{-1}$ ) was used. The difference method (eq 9) provides a marked improvement in accuracy, espe-

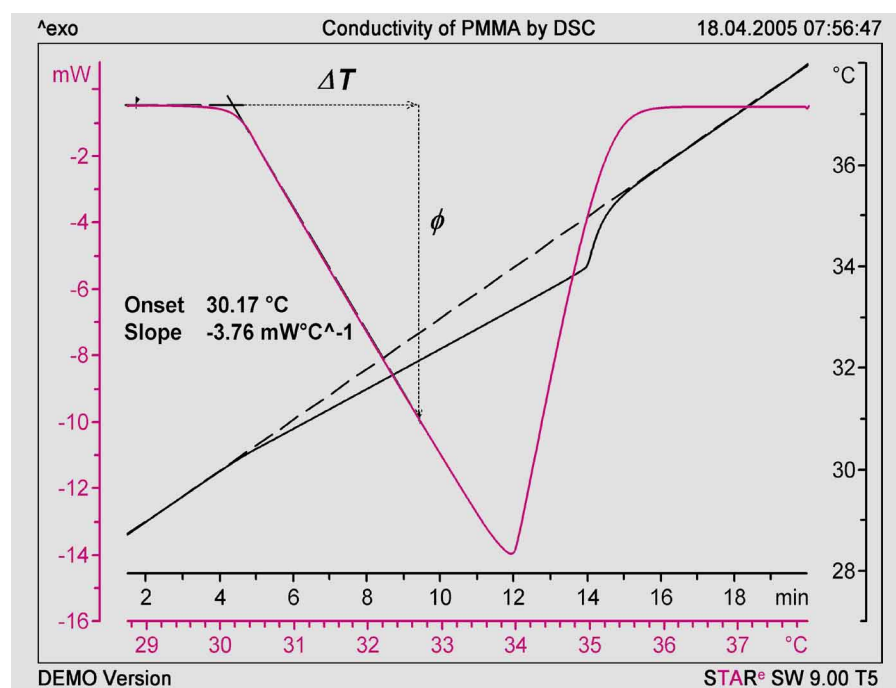


Figure 2. The red curve shows the DSC curve of PMMA (mounted as in Fig. 1) as a function of sample temperature ( $T_s$ ); the black curve the measured sample temperature at the lower end surface of the sample; and the dashed line the program temperature (reference temperature).

Sample	Lit. values	h	D	S	$\lambda$ Direct	Difference to lit.	$\lambda$ Difference	Difference to lit.
	$\text{Wm}^{-1}\text{K}^{-1}$	mm	mm	$\text{mW}\cdot\text{K}^{-1}$	$\text{Wm}^{-1}\text{K}^{-1}$	%	$\text{Wm}^{-1}\text{K}^{-1}$	%
					eq. 6		eq. 9	
only crucible		0	5.80	90.10				
Cork	0.07	1.576	6.28	1.54	0.078	11.9	0.081	15.4
PS	0.16	0.862	6.06	5.09	0.152	-4.9	0.161	0.7
PVC	0.16	1.399	6.16	3.26	0.153	-4.3	0.159	-0.7
ABS	0.17	1.336	6.06	3.28	0.152	-10.6	0.158	-7.2
PP	0.17	1.285	6.16	3.82	0.165	-3.1	0.172	1.2
PMMA	0.20	1.363	6.00	3.76	0.181	-9.6	0.189	-5.7
PA	0.24	1.364	6.25	4.95	0.220	-8.3	0.233	-3.0
PTFE	0.25	1.049	6.14	5.10	0.181	-27.7	0.192	-23.4
PET	0.27	0.382	4.99	10.49	0.205	-24.1	0.232	-14.1
PF	0.30	1.432	6.40	6.00	0.267	-10.9	0.286	-4.6
PE-LD	0.32	1.352	6.20	6.38	0.286	-10.7	0.308	-3.9
<b>Mean value</b>						<b>-9.3</b>		<b>-4.1</b>
<b>Standard deviation</b>						<b>10.5</b>		<b>9.6</b>

Table 2. Thermal conductivity ( $\lambda$ ) of different polymers. " $\lambda$  Direct" was determined from single measurements using eq 6. " $\lambda$  Difference" was determined according to eq 9 from two measurements: the measurement with a sample and the measurement without a sample (only crucible with gallium). The difference with respect to the literature value (Table 1) is given as % of the literature value.

cially for higher conductivities. The mean values and standard deviations compared with the literature values give a good indication of the accuracy and the reproducibility of the methods.

A measurement series with PTFE cylinders of different height shows that the linear

relationship in eq 8 is obeyed (Figure 3). To obtain different cylinder heights, up to nine individual disks were placed on top of one another and the spaces between filled with oil. These measurements show that the degree of scatter of the individual measured values is small. The thermal conductivity of  $0.206 \text{ Wm}^{-1}\text{K}^{-1}$  calculated

from the slope of the regression curve differs only slightly from that found using the difference method ( $\lambda = 0.192 \text{ Wm}^{-1}\text{K}^{-1}$ ).

## Conclusions

The determination of the thermal conductivity of polymers can easily be performed by DSC; the measurement uncertainty is usually less than 20%. The value of -4% obtained for the deviation of the measured values from the literature values is comparable with the result of the interlaboratory study based on ASTM Standard E1952 (-6% mean measurement deviation with a repeatability,  $r$ , of 12%). The standard procedure is based on several temperature-modulated DSC measurements. It requires an accurately known reference substance and the evaluations involve complex mathematical calculations. Despite the significantly greater amount of time and complexity of the ASTM E1952 procedure, the thermal conductivity values measured are not more accurate than those obtained with the simple method used here. Furthermore, only two polymers were measured in the interlaboratory study of the E1952 Standard. Here, in contrast, eleven different materials were measured and a

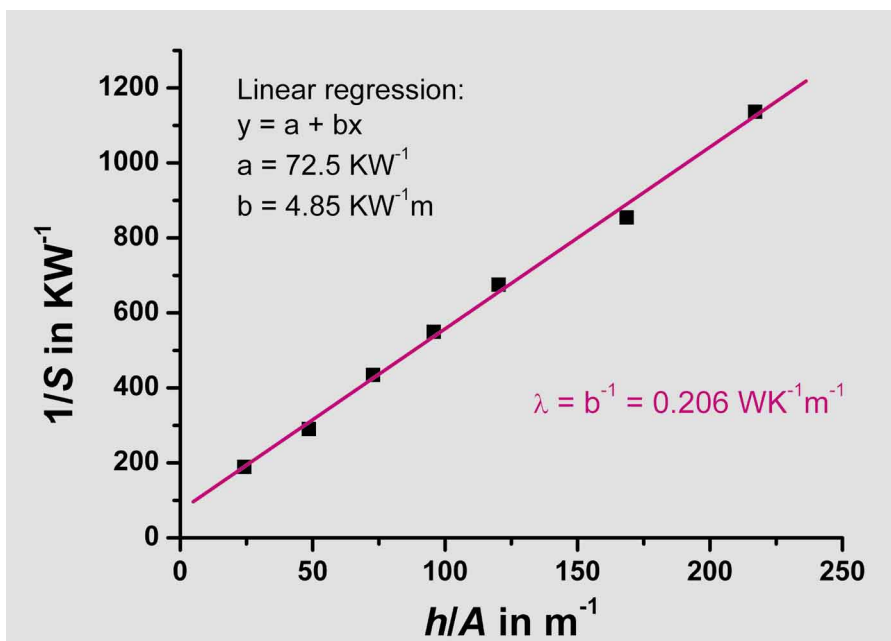


Figure 3. Measurement of different numbers of PTFE disks approx. 0.47 mm thick placed on top of one another, plotted according to eq 8.

much broader thermal conductivity range was determined.

The sample cylinder or disk should be about 1 to 3 mm in height and must have the same diameter as the bottom of the crucible containing the pure metal. In the molten state, the metal must completely cover the bottom of the crucible. If gallium is used as the reference metal, the aluminum crucible must be coated internally with a lacquer in order to prevent alloy formation. The spaces between the sensor and sample and the sample and crucible are

filled with oil so that thermal resistances are as reproducible as possible. Furthermore, the end faces of the sample disks must be flat.

The DSC should be adjusted in the usual way with just the crucible and the metal (i.e. without the cylindrical sample) so that the enthalpy of melting and the melting temperature agree with literature values.

In general, we recommend that you perform the determination according to eq 9, using a measurement with and without the sample.

## Literature

- [1] G. Hakvoort, L. L. Van Reijen, *Thermochimica Acta*, 93 (1985) p 317
- [2] D. M. Price, M. Jarratt, *Thermochimica Acta*, 392-393 (2002) p 231
- [3] C. P. Camirand, *Thermochimica Acta*, 417 (2004) p 1
- [4] H. Saechtling, *Kunststoff Taschenbuch*, 27.Ausgabe, Carl Hanser Verlag, München, 1998
- [5] H. Domininghaus, *Die Kunststoffe and ihre Properties (VDI-Buch)*, Springer-Verlag, Heidelberg, 1986
- [6] ASTM E 1952, ASTM International, West Conshohocken, USA

Note concerning heat transfer oil: Use only good quality oil that leaves no residue when the sensor is baked out at 500 °C.

## Dates

### Exhibitions, Conferences and Seminars – Veranstaltungen, Konferenzen und Seminare

THERMANS 2006	February 6-8, 2006	University of Rajasthan, Jaipur (India)
Analytica 2006	April 25-28, 2006	Munich (Germany)
NATAS 2006	August 6-9, 2006	Bowling Green (Kentucky, USA)
ESTAC9	August 27-31, 2006	Cracow (Poland)

### TA Customer Courses and Seminars in Switzerland – Information and Course Registration:

#### TA-Kundenkurse und Seminare in der Schweiz – Auskunft und Anmeldung bei:

Frau Esther Andreato, Mettler-Toledo GmbH, Analytical, Schwerzenbach, Tel: ++41 44 806 73 57, Fax: ++41 44 806 72 60, e-mail: [esther.andreato@mt.com](mailto:esther.andreato@mt.com)

	Deutsch		English	
	TAK08	TAK44	TAK09	TAK45
SW Basic Course	20.02.2006	30.10.2006	27.02.2006	06.11.2006
TMA Course	20.02.2006	30.10.2006	27.02.2006	06.11.2006
DMA Basic Course	20.02.2006	30.10.2006	27.02.2006	06.11.2006
DMA Advanced Course	21.02.2006	31.10.2006	28.02.2006	07.11.2006
TGA Course	21.02.2006	31.10.2006	28.02.2006	07.11.2006
TGA-MS Course	22.02.2006	01.11.2006	01.03.2006	08.11.2006
DSC Basic Course	22.02.2006	01.11.2006	01.03.2006	08.11.2006
DSC Advanced Course	23.02.2006	02.11.2006	02.03.2006	09.11.2006
TGA-FTIR Course	23.02.2006	02.11.2006	02.03.2006	09.11.2006
SW Advanced Course	24.02.2006	03.11.2006	03.03.2006	10.11.2006

### Cours et séminaires d'Analyse Thermique en France

Renseignements et inscriptions par

Christine Fauvarque, Mettler-Toledo S.A., 18-20 Av. de la pépinière, 78222 Viroflay Cedex, Tél: ++33 1 3097 1439, Fax: ++33 1 3097 1660

Principe de la TMA	2 octobre 2006 Viroflay (France)	Principe de la TGA	5 octobre 2006 Viroflay (France)
Principe de la DSC : les bases	3 octobre 2006 Viroflay (France)	Logiciel STAR <sup>e</sup> : perfectionnement	6 octobre 2006 Viroflay (France)
Principe de la DSC : perfectionnement	4 octobre 2006 Viroflay (France)		

#### Cours à thèmes à Viroflay (France), date : nous consulter

DSC à température modulée (Prof. J.P. Grollier)	L'AT dans les domaines pharmaceutique, cosmétique et biologique (Prof. J.M. Létoffe)
Vieillessement des polymères (Prof. M. Baba)	
La cinétique appliquée à l'Analyse Thermique (Prof. N. Sbirrazzuoli)	L'AT appliquée à l'industrie pétrolière (Prof. J.M. Létoffe)
La sécurité des procédés : la DSC un outil indispensable (Prof. F. Stoessel)	L'AT et la caractérisation des polymères (Prof. J.M. Létoffe)

